Vietnam Journal of Mathematics manuscript No.
(will be inserted by the editor)

On the scalability of classical one-level domain-decomposition methods

F. Chaouqui[1] · **G. Ciaramella**[2] · **M. J. Gander**[1] · **T. Vanzan**[1]

the date of receipt and acceptance should be inserted later

Abstract One-level domain decomposition methods are in general not scalable, and coarse corrections are needed to obtain scalability. It has however recently been observed in applications in computational chemistry that the classical one-level parallel Schwarz method is surprizingly scalable for the solution of one- and two-dimensional chains of fixed-sized subdomains. We first review some of these recent scalability results of the classical one-level parallel Schwarz method, and then prove similar results for other classical one-level domain-decomposition methods, namely the optimized Schwarz method, the Dirichlet-Neumann method, and the Neumann-Neumann method. We show that the scalability of one-level domain decomposition methods depends critically on the geometry of the domain decomposition and the boundary conditions imposed on the original problem. We illustrate all our results also with numerical experiments.

Keywords domain-decomposition methods; scalability; classical and optimized Schwarz methods; Dirichlet-Neumann method; Neumann-Neumann method; solvation model; chain of atoms; Laplace's equation.

AMS Classification 65N55, 65F10, 65N22, 70-08, 35J05, 35J57.

1 Introduction

Recent developments in physical and chemical applications are creating a large demand for numerical methods for the solution of complicated systems of equations, which are often used before rigorous numerical analysis results are available. Moreover, the nature of the applications makes such systems untreatable by sequential algorithms and generates the need of methods that are parallel in nature or that can be easily parallelized.

In the field of parallel methods an important role is played by the so-called "scalability property" of an algorithm. An algorithm is "strongly scalable", if the acceleration generated by the parallelization scales proportionally with the number of processors that are used. For example if on 10 processors, a strongly scalable algorithm needs 10 seconds to solve

Work supported by ...

[1] Section de mathématiques, Université de Genève, 2-4 rue du Lièvre, Genève,
[2] Fachbereich Mathematik und Statistik, University of Constance, Germany.

the problem, it would need 1 second using 100 processors. Strong scalability is difficult to achieve, because eventually there is not enough work left to do for each processor and communication dominates, but it is possible up to some point, see for instance Table 1 in [30] and Table 3 in [23]. One therefore also talks about “weak scalability”, which means that one can solve a larger and larger problem with more and more processors in a fixed amount of time. For example, if a weakly scalable algorithm solves a problem with 100’000 unknowns in 10 seconds using 10 processors, it should be able to solve a problem with 1’000’000 unknowns in the same 10 seconds using 100 processors. In particular, a domain-decomposition method is said to be weakly scalable, if its rate of convergence does not deteriorate when the number of subdomains grows [40].

To analyze weak scalability, we study in this paper the contraction (or convergence) factor ρ of the algorithms, the convergence rate being $-\log\rho$, see [27, Section 11.2.5]. Thus if the contraction factor of a method does not deteriorate, also the convergence rate does not deteriorate and the method is weakly scalable. To explain now what the contraction factor ρ of a stationary iterative method is, we assume that it generates for iteration index $0,1,2,\dots$ an error sequence $\mathbf{e}^0,\mathbf{e}^1,\mathbf{e}^2,\dots$ converging geometrically in a given norm $\|\cdot\|$, that is $\frac{\|\mathbf{e}^n\|}{\|\mathbf{e}^0\|}\leq\rho^n$, and ρ is the associated contraction factor. Now, assume that the iterative procedure stops at a given tolerance $\texttt{Tol}$, that is $\frac{\|\mathbf{e}^n\|}{\|\mathbf{e}^0\|}\approx\texttt{Tol}$. By combining these two formulas we get $\texttt{Tol}\approx\frac{\|\mathbf{e}^n\|}{\|\mathbf{e}^0\|}\leq\rho^n$, and estimate the number of iterations necessary to achieve $\texttt{Tol}$ as $n\leq\frac{|\log\texttt{Tol}|}{|\log\rho|}$. If the contraction factor ρ of a domain decomposition method is uniformly bounded by a constant strictly less than one, independently of the number of subdomains N, then the method converges to a given tolerance with a number of iterations n that is independent of the number of subdomains N, and the method is thus weakly scalable: its convergence rate $-\log\rho$ can not deteriorate when the number of subdomains grows. We study therefore in Sections 3,4,5 and 6 the contraction factors for different domain decomposition methods, and we provide a constant bound strictly less than one which is independent of the number of subdomains N, provided that size of the subdomains is fixed, which is a sufficient condition for the domain decomposition methods to be weakly scalable.

As a particular example of this weak-scalability behavior, we recall the new methodology that was recently presented in [3] and supported by [34,35]. Based on a physical approximation of solvation phenomena [1,29,41], the authors introduced a new formulation of the Schwarz domain-decomposition methods for the solution of solvation problems, where large molecular systems, given by chains of atoms, are involved. Each atom corresponds in this formulation to a subdomain, and the Schwarz methods are written in a boundary element form. The authors have observed in their numerical experiments the surprising result that the convergence of the iterative procedure without coarse correction is in many cases independent of the number of atoms and thus subdomains, which means that simple one-level Schwarz (alternating and parallel) methods for the solution of chains of particles are weakly scalable; no coarse correction seems to be necessary. On the other hand, it is well known that the convergence of Schwarz methods without coarse correction depends in general for elliptic problems on the number of subdomains, see for example [40]. The surprising scalability result of the classical one-level Schwarz method in the special case of a chain of atoms was recently explained using three different types of analysis: in [6], the authors used Fourier analysis for an approximate 2-dimensional model that describes a chain of atoms whose domains are approximated by rectangles; in [7], the maximum principle was used for more realistic 2-dimensional chains of atoms; in [8] the unusual scaling behavior was explained using variational methods. These scalability results represent exceptions to the classical Schwarz theory [40], which shows that one-level domain-decomposition

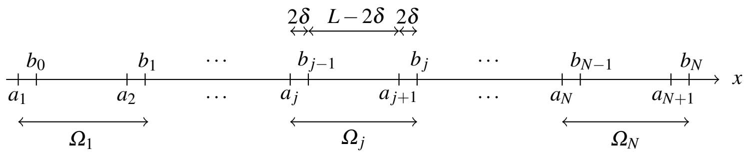

Fig. 1 One-dimensional chain of N fixed-sized subdomains of length $L+2\delta$. The overlap is 2δ.

methods are in general not scalable. Two-level domain-decomposition methods, i.e. domain-decomposition methods with coarse corrections, attempt to reach this goal; see the seminal contributions [37,10], and [12] for FETI, and more generally the books [39,38,40] and references therein. Coarse spaces were also developed for optimized Schwarz methods, see the first contribution [11], and [17], which is based on the new idea of optimal coarse spaces and their approximation from [16], see [19] for a general introduction. Optimal coarse spaces lead to convergence in a finite number of iterations [4], i.e. the method becomes nilpotent, and for certain decompositions and methods this is even possible without coarse space, see [5]. Based on the optimal coarse space, optimized variants were developed in [18] for restricted additive Schwarz, in [24] for additive Schwarz, and in [21,20] for multiscale problems, including a condition number estimate.

At this point it seems natural to ask: is it possible for other classical domain decomposition methods to be scalable without coarse correction, like Dirichlet-Neumann methods, Neumann-Neumann methods, and optimized Schwarz methods ? Answering this question is the main goal of this paper. We focus on the Laplace equation defined on one- and two-dimensional chains of subdomains introduced in Section 2, because scalability depends on the dimension and the boundary conditions. We then define the parallel Schwarz method for the solution to these models in Section 3, and review the scalability results from [6]. In Section 4, we prove that also optimized Schwarz methods have the same scalability properties, and this even without overlap. Section 5 focuses on the scalability analysis of the Dirichlet-Neumann method, and Section 6 on the Neumann-Neumann method. In all cases, we prove that these one-level methods can be scalable for certain geometric situations and boundary conditions. We illustrate our analysis with numerical experiments in Section 7.

2 Formulation of the problem: growing chains of fixed-sized subdomains

In this section, we define our model problems consisting of chains of N subdomains in one and two spatial dimensions, which we will use to study classical one-level domain-decomposition methods. In particular, we are interested in the behavior of these methods when the number N of subdomains grows while their size is fixed.

We begin describing the one-dimensional problem. Consider the domain $\Omega=(a_1,b_N)$ shown in Figure 1, where the two extrema are the first and the last elements of two sets of points a_j, for $j=1,\dots,N+1$, and b_j, for $j=0,\dots,N$, defined as $a_j:=(j-1)L-\delta$ and $b_j:=jL+\delta$. Therefore, a_j and b_j form a grid in Ω and define the subdomains $\Omega_j:=(a_j,b_j)$ such that $\Omega=\cup_{j=1}^{N}\Omega_j$. The quantities $L>0$ and $\delta>0$ parametrize the dimension of each subdomain Ω_j and the overlap $\Omega_j\cap\Omega_{j+1}$ whose length is 2δ. We are interested in the solution to the problem

$$-\Delta u=f \text{ in } \Omega,\; u(a_1)=g_1,\; u(b_N)=g_N, \tag{1}$$

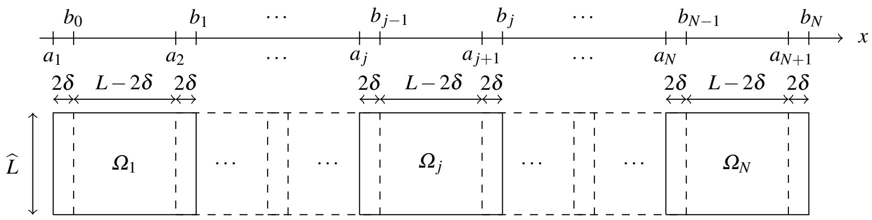

Fig. 2 Two-dimensional chain of N rectangular fixed-sized subdomains.

where f is a sufficiently regular function and $g_1, g_N \in \mathbb{R}$. Problem (1) can be formulated as follows: we introduce the function u_j as the restriction of u to Ω_j. Hence u_j satisfies

$$\begin{aligned} -\Delta u_j &= f_j \quad \text{in } \Omega_j,\\ u_j &= u_{j-1} \ \text{ in } [a_j, b_{j-1}],\\ u_j &= u_{j+1} \ \text{ in } [a_{j+1}, b_j], \end{aligned} \tag{2}$$

where the last two conditions describe the interaction of the j-th subdomain with subdomains $j-1$ and $j+1$, and the function f_j is the restriction of f to Ω_j. Notice that problem (2) is defined for $j = 2, \ldots, N-1$. The functions u_1 and u_N of the first and the last subdomains solve

$$\begin{aligned} -\Delta u_1 &= f_1 \text{ in } \Omega_1, & -\Delta u_N &= f_N \quad \text{in } \Omega_N,\\ u_1(a_1) &= g_1, & u_N(b_N) &= g_N,\\ u_1 &= u_2 \text{ in } [a_2, b_1], & u_N &= u_{N-1} \text{ in } [a_N, b_{N-1}]. \end{aligned} \tag{3}$$

Now we consider the two-dimensional model. To define each subdomain, let us consider $L > 0$ and $\delta > 0$, and define the grid points a_j for $j = 1, \ldots, N+1$ and b_j for $j = 0, \ldots, N$ as shown in Figure 2. The j-th subdomain of the chain is a rectangle of dimension $\Omega_j := (a_j, b_j) \times (0, \widehat{L})$. Therefore, the domain of the chain is $\Omega = \cup_{j=1}^{N} \Omega_j$. As before 2δ is the overlap and $\delta \in (0, L/2)$. We are interested in the solution to

$$-\Delta u = f \ \text{ in } \Omega, \quad u = g \ \text{ on } \partial\Omega,$$

where f and g are sufficiently regular functions. We consider f_j and g_j as the restriction of f and g to the j-th subdomain. The restriction of u to Ω_j, denoted by u_j, solves the problem

$$\begin{aligned} -\Delta u_j &= f_j \text{ in } \Omega_j,\\ u_j(\cdot, 0) &= g_j(\cdot, 0),\\ u_j(\cdot, \widehat{L}) &= g_j(\cdot, \widehat{L}),\\ u_j &= u_{j-1} \ \text{ in } [a_j, b_{j-1}] \times (0, \widehat{L}),\\ u_j &= u_{j+1} \ \text{ in } [a_{j+1}, b_j] \times (0, \widehat{L}), \end{aligned} \tag{4}$$

for $j = 2, \ldots, N-1$, and

$$\begin{aligned} -\Delta u_1 &= f_1 \text{ in } \Omega_1, & -\Delta u_N &= f_N \text{ in } \Omega_N,\\ u_1(\cdot, 0) &= g_1(\cdot, 0), & u_N(\cdot, 0) &= g_N(\cdot, 0),\\ u_1(\cdot, \widehat{L}) &= g_1(\cdot, \widehat{L}), & u_N(\cdot, \widehat{L}) &= g_N(\cdot, \widehat{L}),\\ u_1(a_1, \cdot) &= g_1(a_1, \cdot), & u_N(b_N, \cdot) &= g_N(b_N, \cdot),\\ u_1 &= u_2 \text{ in } [a_2, b_1] \times (0, \widehat{L}), & u_N &= u_{N-1} \text{ in } [a_N, b_{N-1}] \times (0, \widehat{L}). \end{aligned} \tag{5}$$

The two models presented in this section seem to be very similar because of their main one-dimensional structure (the subdomains are aligned along a straight line). However, we will see in the following sections that they lead to completely different convergence behavior of domain-decomposition methods.

3 Classical parallel Schwarz method

In this section, we study the convergence of the classical parallel Schwarz method (PSM), in the form introduced by Lions in [31], for the problems presented in Section 2. In particular, we analyze the behavior of the PSM for a growing number of (fixed-sized) subdomains and investigate the corresponding weak scalability. We show that the PSM for the solution of the one-dimensional problem (2)-(3) is not scalable, in the sense that the spectral radius ρ of the iteration matrix tends to one as N grows. On the other hand, for the two-dimensional problem (4)-(5), we prove that there exists a function $\bar{\rho}$, independent of N and such that $\rho \leq \bar{\rho} < 1$, which means that the PSM is scalable.

3.1 One-dimensional analysis

Consider problem (2)-(3) and an initial guess $u_1^0, u_2^0, \dots, u_N^0$. The PSM defines the approximation sequences $\{u_j^n\}_n$ by solving

$$\begin{aligned} -\partial_{xx} u_j^n &= f_j \text{ in } (a_j, b_j), \\ u_j^n(a_j) &= u_{j-1}^{n-1}(a_j), \\ u_j^n(b_j) &= u_{j+1}^{n-1}(b_j), \end{aligned}$$

for $j = 2, \dots, N-1$, and

$$\begin{aligned} -\partial_{xx} u_1^n &= f_1 \text{ in } (a_1, b_1), & -\partial_{xx} u_N^n &= f_N \text{ in } (a_N, b_N), \\ u_1^n(a_1) &= 0, & u_N^n(a_N) &= u_{N-1}^{n-1}(a_N), \\ u_1^n(b_1) &= u_2^{n-1}(b_1), & u_N^n(b_N) &= 0. \end{aligned}$$

To analyze the convergence of this algorithm, we introduce the errors $e_j^n := u_j - u_j^n$ and notice that they satisfy

$$\begin{aligned} -\partial_{xx} e_j^n &= 0 \text{ in } (a_j, b_j), \\ e_j^n(a_j) &= e_{j-1}^{n-1}(a_j), \\ e_j^n(b_j) &= e_{j+1}^{n-1}(b_j), \end{aligned} \tag{6}$$

for $j = 2, \dots, N-1$, and

$$\begin{aligned} -\partial_{xx} e_1^n &= 0 \text{ in } (a_1, b_1), & -\partial_{xx} e_N^n &= 0 \text{ in } (a_N, b_N), \\ e_1^n(a_1) &= 0, & e_1^n(a_N) &= e_{N-1}^{n-1}(a_N), \\ e_1^n(b_1) &= e_2^{n-1}(b_1), & e_1^n(b_N) &= 0. \end{aligned} \tag{7}$$

The convergence of (6) and (7) can be established via an analysis based on the maximum principle; see, e.g. [32,7]. Since this analysis reveals that the PSM is not scalable, we sketch

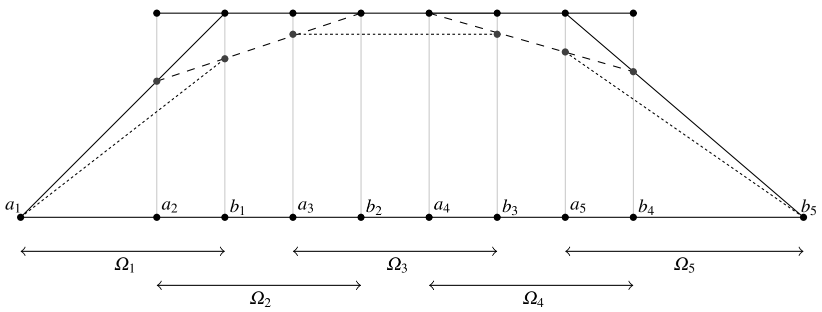

Fig. 3 Example of the PSM for a chain of $N=5$ subdomains. The solid lines are the errors at the first iteration e_j^1, the dashed lines represent e_j^2, and the dotted line is e_3^3. It is possible to observe that the contraction of the error propagates from the first and the last subdomains (Ω_1 and Ω_5) till the middle subdomain Ω_3. To reach Ω_3, the propagation needs 3 iterations.

it in what follows for the example in Figure 3. Let us consider an initial error $e^0 = 1$. The solutions of the internal subdomains is $e_j^1 = 1$ for $j = 2, \dots, 4$, whereas the solutions of the first and the last subdomains are straight lines that have value 1 on the interface points b_1 and a_5 and that are zero on a_1 and b_5 (solid lines in Figure 3). Therefore, at the interface points a_2 and b_4 the error is strictly smaller than 1, a result that holds in general for equations that satisfy a maximum principle. This means that at the second iteration, the errors e_2^2 and e_4^2 (dashed lines in Figure 3) are straight lines such that $e_2^2(a_2) = e_1^1(a_2) < 1$ and $e_2^2(b_2) = e_3^1(b_2) = 1$, and $e_4^2(b_4) = e_5^1(b_4) < 1$ and $e_4^2(a_4) = e_3^1(a_4) = 1$, whereas the errors on the subdomains Ω_1, Ω_3, and Ω_5 do not change ($e_1^2 = e_1^1$, $e_3^2 = e_3^1$, and $e_5^2 = e_5^1$). Hence, we observe a contraction of the error in Ω_2 and Ω_4, but the error $e_3^2 = 1$ is still not contracting. At the third iteration, we observe a contraction on Ω_1 and Ω_5 and, finally, also on Ω_3, because at the points a_3 and b_3 it holds that $e_3^3(a_3) = e_2^2(a_3) < 1$ and $e_3^3(b_3) = e_4^2(b_3) < 1$, which implies by the maximum principle that $e_3^3(x) < 1$ (dotted lines in Figure 3). This example shows that, to observe a contraction in the subdomain in the middle of the chain, that is Ω_3, we have to wait 3 iterations. By induction, we thus have to wait about $N/2$ iterations before observing a contraction of the error in the subdomains in the middle of the chain. Hence, for a growing number of subdomains N one has to wait more and more iterations before the error contracts on each subdomain in the chain. This observation indicates that the PSM for the solution of the one-dimensional problem (2)-(3) is not scalable.

We study now in detail the convergence of the PSM (6)-(7), whose solutions are

$$e_j^n(x) = e_{j-1}^{n-1}(a_j) + \frac{x-a_j}{b_j-a_j}\left(e_{j+1}^{n-1}(b_j) - e_{j-1}^{n-1}(a_j)\right),$$

for $j = 2, \dots, N-1$, and

$$e_1^n(x) = \frac{x-a_1}{b_1-a_1} e_2^{n-1}(b_1), \qquad e_N^n(x) = \Big(1 - \frac{x-a_N}{b_N-a_N}\Big) e_{N-1}^{n-1}(a_N).$$

Evaluating e_j^n at the interface points and defining the vector

$$\mathbf{e}^n := \big[0\,,\, e_2^n(b_1)\,,\, e_1^n(a_2)\,,\, e_3^n(b_2)\,,\, \cdots\,,\, e_{j-1}^n(a_j)\,,\, e_{j+1}^n(b_j)\,,\, \cdots\,,$$
$$e_{N-2}^n(a_{N-1})\,,\, e_N^n(b_{N-1})\,,\, e_{N-1}^n(a_N)\,,\, 0\big]^\top,$$

we get

$$\mathbf{e}^n = T_{1D}\mathbf{e}^{n-1},$$

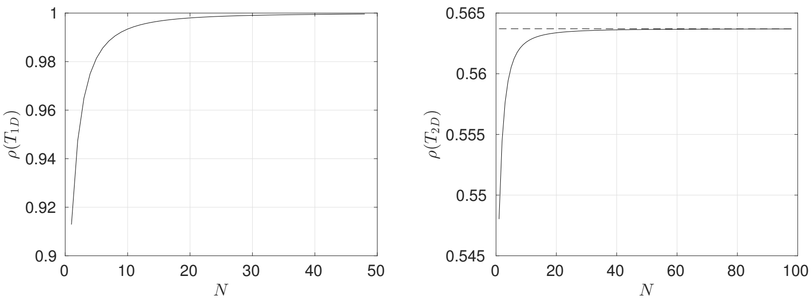

Fig. 4 Left: spectral radius of the iteration matrix T_{1D} corresponding to $\delta = 0.1$ and $L = 1$. It is clear that $\rho(T_{1D}) \to 1$ for growing N. Right: spectral radius (solid line) and infinity-norm (dashed line) of the matrix T_{2D} corresponding to $L = 1$, $\widehat{L} = 1$, $\delta = 0.1$, and $k = \pi$. Notice that $\rho(T_{2D})$ does not deteriorates as N grows.

where the (block) matrix T_{1D} is given by

$$T_{1D} := \begin{bmatrix} & T_2 & & & & & & \\ \widetilde{T}_1 & & T_2 & & & & & \\ & T_1 & & T_2 & & & & \\ & & T_1 & & T_2 & & & \\ & & & \ddots & & \ddots & & \\ & & & & T_1 & & T_2 & \\ & & & & & T_1 & & \widetilde{T}_2 \\ & & & & & & T_1 & \end{bmatrix}, \tag{8}$$

whose blocks are

$$T_1 := \begin{bmatrix} \frac{2\delta}{2\delta+L} & \frac{L}{2\delta+L} \\ 0 & 0 \end{bmatrix},\ T_2 := \begin{bmatrix} 0 & 0 \\ \frac{L}{2\delta+L} & \frac{2\delta}{2\delta+L} \end{bmatrix},\ \widetilde{T}_1 := \begin{bmatrix} 0 & \frac{L}{2\delta+L} \\ 0 & 0 \end{bmatrix},\ \widetilde{T}_2 := \begin{bmatrix} 0 & 0 \\ \frac{L}{2\delta+L} & 0 \end{bmatrix}.$$

To study the convergence of the sequence $\{\mathbf{e}^n\}_n$ we compute numerically the spectral radius of the iteration matrix T_{1D}, denoted by $\rho(T_{1D})$. In particular, we fix a value of the overlap δ and compute $\rho(T_{1D})$ for growing N. This is shown in Figure 4 (left), where the spectral radius is bounded by 1 for any N and $\rho(T_{1D}) \to 1$ as N grows. Therefore, the PSM for the solution of the one-dimensional problem is not weakly scalable because $\rho(T_{1D})$ deteriorates as N grows. To explain the bound $\rho(T_{1D}) \leq 1$, we assume that $N \geq 5$ (to obtain exactly the structure of T_{1D} given in (8)), recall that $\rho(T_{1D}) \leq \|T_{1D}\|_\infty$ and notice that

$$\|T_{1D}\|_\infty = \max\big\{ \|T_1 + T_2\|_\infty , \|\widetilde{T}_1 + T_2\|_\infty , \|T_1 + \widetilde{T}_2\|_\infty \big\},$$

since all the entries of T_1, T_2, $\widetilde{T}_1$, and $\widetilde{T}_2$ are positive. Observing that

$$\|T_1 + T_2\|_\infty = \|\widetilde{T}_1 + T_2\|_\infty = \|T_1 + \widetilde{T}_2\|_\infty = 1,$$

we conclude that $\rho(T_{1D}) \leq \|T_{1D}\|_\infty = 1$.

3.2 Two-dimensional analysis

In this section, we study the PSM for the solution to (4)-(5). The analysis we present is mainly based on the results obtained in [6], but we consider a different construction of the iteration matrix, which is similar to the one considered for the other methods in the following sections. The PSM is given by

$$\begin{aligned} -\Delta u_j^n &= f_j \text{ in } \Omega_j, \\ u_j^n(\cdot,0) &= g_j(\cdot,0), \\ u_j^n(\cdot,\widehat{L}) &= g_j(\cdot,\widehat{L}), \\ u_j^n(a_j,\cdot) &= u_{j-1}^{n-1}(a_j,\cdot), \\ u_j^n(b_j,\cdot) &= u_{j+1}^{n-1}(b_j,\cdot), \end{aligned}$$

for $j = 2,\dots,N-1$, and

$$\begin{aligned} -\Delta u_1^n &= f_1 \quad \text{in } \Omega_1, & -\Delta u_N^n &= f_N \quad \text{in } \Omega_N, \\ u_1^n(\cdot,0) &= g_1(\cdot,0), & u_N^n(\cdot,0) &= g_N(\cdot,0), \\ u_1^n(\cdot,\widehat{L}) &= g_1(\cdot,\widehat{L}), & u_N^n(\cdot,\widehat{L}) &= g_N(\cdot,\widehat{L}), \\ u_1^n(a_1,\cdot) &= g_1(a_1,\cdot), & u_N^n(a_N,\cdot) &= u_{N-1}^{n-1}(a_N,\cdot), \\ u_1^n(b_1,\cdot) &= u_2^{n-1}(b_1,\cdot), & u_N^n(b_N,\cdot) &= g_N(b_N,\cdot). \end{aligned}$$

Introducing again the errors $e_j^n := u_j - u_j^n$, the PSM becomes

$$\begin{aligned} -\Delta e_j^n &= 0 \text{ in } \Omega_j, \\ e_j^n(\cdot,0) &= 0,\ e_j^n(\cdot,\widehat{L}) = 0, \\ e_j^n(a_j,\cdot) &= e_{j-1}^{n-1}(a_j,\cdot), \\ e_j^n(b_j,\cdot) &= e_{j+1}^{n-1}(b_j,\cdot), \end{aligned} \tag{9}$$

for $j = 2,\dots,N-1$, and

$$\begin{aligned} -\Delta e_1^n &= 0 \quad \text{in } \Omega_1, & -\Delta e_N^n &= 0 \quad \text{in } \Omega_N, \\ e_1^n(\cdot,0) &= 0,\ e_1^n(\cdot,\widehat{L}) = 0, & e_N^n(\cdot,0) &= 0,\ e_N^n(\cdot,\widehat{L}) = 0, \\ e_1^n(a_1,\cdot) &= 0, & e_N^n(a_N,\cdot) &= e_{N-1}^{n-1}(a_N,\cdot), \\ e_1^n(b_1,\cdot) &= e_2^{n-1}(b_1,\cdot), & e_N^n(b_N,\cdot) &= 0. \end{aligned} \tag{10}$$

To construct the Schwarz iteration matrix corresponding to (9)-(10), we use the Fourier sine expansion

$$e_j^n(x,y) = \sum_{m=1}^{\infty} v_j^n(x,k)\sin(ky), \quad k = \frac{\pi m}{\widehat{L}},$$

where the Fourier coefficients $v_j^n(x,k)$ are given by

$$v_j^n(x,k) = \widetilde{c}_j(k,\delta)e^{kx} + \widetilde{d}_j(k,\delta)e^{-kx},$$

and $\widetilde{c}_j(k,\delta)$ and $\widetilde{d}_j(k,\delta)$ are computed using the conditions $v_j^n(a_j,k) = v_{j-1}^{n-1}(a_j,k)$ and $v_j^n(b_j,k) = v_{j+1}^{n-1}(b_j,k)$, which are obtained by using the transmission conditions. Notice that k is parametrized by m, hence one should formally write k_m, but we drop the subscript m for simplicity. For $j = 2,\dots,N-1$, we obtain that

$$\begin{aligned} v_j^n(x,k) = e^{kx}e^{-jkL}\Big[g_{A1}(k,\delta)v_{j+1}^{n-1}(b_j,k) - g_{A2}(k,\delta)v_{j-1}^{n-1}(a_j,k)\Big] \\ + e^{-kx}e^{jkL}\Big[g_{B1}(k,\delta)v_{j-1}^{n-1}(a_j,k) - g_{B2}(k,\delta)v_{j+1}^{n-1}(b_j,k)\Big] \end{aligned} \tag{11}$$

with

$$\begin{aligned} g_{A1}(k,\delta) &:= \frac{e^{3k\delta+2kL}}{e^{4k\delta+2kL}-1}, \quad g_{A2}(k,\delta) := \frac{e^{k\delta+kL}}{e^{4k\delta+2kL}-1}, \\ g_{B1}(k,\delta) &:= \frac{e^{3k\delta+kL}}{e^{4k\delta+2kL}-1}, \quad g_{B2}(k,\delta) := \frac{e^{k\delta}}{e^{4k\delta+2kL}-1}. \end{aligned}$$

We rewrite (11) in the form

$$v_j^n(x,k) = w_j(x,k;\delta)v_{j+1}^{n-1}(b_j,k) + z_j(x,k;\delta)v_{j-1}^{n-1}(a_j,k), \tag{12}$$

where

$$\begin{aligned} w_j(x,k;\delta) &:= e^{kx}e^{-jkL}g_{A1}(k,\delta) - e^{-kx}e^{jkL}g_{B2}(k,\delta), \\ z_j(x,k;\delta) &:= e^{-kx}e^{jkL}g_{B1}(k,\delta) - e^{kx}e^{-jkL}g_{A2}(k,\delta). \end{aligned}$$

In a similar fashion, solving problems (10), we get

$$v_1^n(x,k) = w_1(x,k;\delta)v_2^{n-1}(b_1,k), \quad v_N^n(x,k) = z_N(x,k;\delta)v_{N-1}^{n-1}(a_N,k),$$

with

$$\begin{aligned} w_1(x,k;\delta) &:= \frac{e^{k\delta+kL}}{1-e^{4k\delta+2kL}}\left[e^{-kx} - e^{2k\delta+kx}\right], \\ z_N(x,k;\delta) &:= \frac{e^{k\delta+kL}}{1-e^{4k\delta+2kL}}\left[e^{kx-kNL} - e^{kNL+2k\delta-kx}\right]. \end{aligned}$$

Now, we define

$$\begin{aligned} w_a(k,\delta) &:= w_j(a_{j+1},k;\delta) = w_{j-1}(a_j,k;\delta), \\ w_b(k,\delta) &:= w_{j+1}(b_j,k;\delta) = w_j(b_{j-1},k;\delta), \\ z_a(k,\delta) &:= z_j(a_{j+1},k;\delta) = z_{j-1}(a_j,k;\delta), \\ z_b(k,\delta) &:= z_{j+1}(b_j,k;\delta) = z_j(b_{j-1},k;\delta), \end{aligned} \tag{13}$$

and a direct calculation [6] shows that $z_b(k,\delta) = \frac{e^{2k\delta+2kL}-e^{2k\delta}}{e^{4k\delta+2kL}-1}$, $w_b(k,\delta) = \frac{e^{4k\delta+kL}-e^{kL}}{e^{4k\delta+2kL}-1}$, with

$$(z_b + w_b)(k,\delta) = \frac{e^{2k\delta}+e^{kL}}{e^{2k\delta+kL}+1}. \tag{14}$$

We recall the following results [6, Lemma 1 and Lemma 2].

Lemma 1 *For any $(k,\delta) \in (0,\infty)\times[0,L]$, the quantities defined in* (13) *satisfy $w_a(k,\delta) \geq 0$ and $w_b(k,\delta) \geq 0$. Moreover $w_a(k,\delta) = z_b(k,\delta)$ and $w_b(k,\delta) = z_a(k,\delta)$.*

Lemma 2 *The following statements hold:*

(a) *For any* $\delta > 0$*, the map* $k \in (0,\infty) \mapsto (z_b + w_b)(k,\delta) \in \mathbb{R}$ *is strictly monotonically decreasing.*
(b) *For any* $k > 0$*, the map* $\delta \in (0, L/2) \mapsto (z_b + w_b)(k,\delta) \in \mathbb{R}$ *is strictly monotonically decreasing.*
(c) *For any* $k > 0$*, we have* $(z_b + w_b)(k,0) = 1$*,* $\frac{\partial(z_b+w_b)}{\partial k}(k,0) = 0$ *and* $\frac{\partial(z_b+w_b)}{\partial \delta}(k,0) < 0$.

Using (12), we evaluate $v_{j-1}^n(x,k)$ and $v_{j+1}^n(x,k)$ at $x = a_j$ and $x = b_j$, define the vector

$$\mathbf{v}^n := \big[0\,, v_2^n(b_1,k)\,, v_1^n(a_2,k)\,, v_3^n(b_2,k)\,, \cdots, v_{j-1}^n(a_j,k)\,, v_{j+1}^n(b_j,k)\,, \cdots, \\ v_{N-2}^n(a_{N-1},k)\,, v_N^n(b_{N-1},k)\,, v_{N-1}^n(a_N,k)\,, 0\big]^\top,$$

and obtain that

$$\mathbf{v}^n = T_{2D}\mathbf{v}^{n-1},$$

where the matrix T_{2D} is given by

$$T_{2D} := \begin{bmatrix} & T_2 & & & & & & & \\ \widetilde{T}_1 & & T_2 & & & & & & \\ & T_1 & & T_2 & & & & & \\ & & T_1 & & T_2 & & & & \\ & & & \ddots & & \ddots & & & \\ & & & & T_1 & & T_2 & & \\ & & & & & T_1 & & \widetilde{T}_2 & \\ & & & & & & T_1 & & \end{bmatrix},$$

whose blocks T_1, T_2, $\widetilde{T}_1$, and $\widetilde{T}_2$ are

$$T_1 := \begin{bmatrix} w_b & z_b \\ 0 & 0 \end{bmatrix}, \quad T_2 := \begin{bmatrix} 0 & 0 \\ z_b & w_b \end{bmatrix}, \quad \widetilde{T}_1 := \begin{bmatrix} 0 & z_b \\ 0 & 0 \end{bmatrix}, \quad \widetilde{T}_2 := \begin{bmatrix} 0 & 0 \\ z_b & 0 \end{bmatrix}.$$

Notice that T_{2D} depends on the overlap parameter δ and the Fourier mode k, but we omitted this dependence for brevity. Now, we bound the spectral radius $\rho(T_{2D})$ by estimating the infinity-norm of T_{2D}. Since Lemma 1 guarantees that w_b and z_b are non-negative, we have that

$$\|T_{2D}\|_\infty = \max\big\{\|T_1 + T_2\|_\infty\,, \|\widetilde{T}_1 + T_2\|_\infty\,, \|T_1 + \widetilde{T}_2\|_\infty\big\},$$

and observe that

$$\|T_1 + T_2\|_\infty = \|\widetilde{T}_1 + T_2\|_\infty = \|T_1 + \widetilde{T}_2\|_\infty = w_b + z_b =: \rho(k,\delta).$$

Recalling (14), Lemma 2, and defining $\bar{\rho}(\delta) := \rho(\frac{\pi}{L},\delta)$, we conclude that $\|T_{2D}\|_\infty \le \rho(k,\delta) \le \bar{\rho}(\delta) < 1$. We summarize this result in the following theorem, which is an analog of [6, Theorem 3].

Theorem 1 *For any* $(k,\delta) \in (0,\infty) \times (0, \frac{L}{2})$ *we have the bound*

$$\rho(T_{2D}(k,\delta)) \le \|T_{2D}(k,\delta)\|_\infty \le \bar{\rho}(\delta) < 1,$$

where $\rho(T_{2D}(k,\delta))$ *is the spectral radius of* $T_{2D}(k,\delta)$ *and* $\bar{\rho}(\delta) := \rho(\frac{\pi}{L},\delta)$*, which is independent of the number N of subdomains. Moreover, for* $N \ge 3$ *it holds that* $\|T_{2D}(k,\delta)\|_\infty = \rho(k,\delta)$.

Theorem 1 shows that the PSM for the solution of the two-dimensional problem converges and the spectral radius (its contraction factor) does not deteriorate as N grows, because $\rho(T_{2D}(k,\delta)) \leq \|T_{2D}(k,\delta)\|_\infty \leq \bar{\rho}(\delta) < 1$ for any N. This means that the PSM for the solution of the two-dimensional problem is weakly scalable. In Figure 4 (right) the spectral radius $\rho(T_{2D})$ (blue line) and the norm $\|T_{2D}\|_\infty$ (red line) are shown as a function of N: as N increases, the spectral radius grows, but it is bounded by the infinity-norm which is strictly smaller than one.

4 Optimized Schwarz method

The classical Schwarz method, despite its flexibility and generality, has major drawbacks such as the requirement of overlap, lack of convergence for some PDEs and slow convergence speed in general [14]. In the pioneering paper [33], Lions proposed to exploit (generalized) Robin conditions as transmission conditions on the interfaces between subdomains to obtain a convergent Schwarz method without overlap. To improve the convergence behavior, one can optimize the Robin parameter, as it was shown in [28]. The generalization of this idea led to overlapping and non-overlapping optimized Schwarz methods (OSMs), which have extensively been studied over the last decades, see [13] for a review, [22] for Helmholtz problems, [9] for Maxwell equations and [26] for advection diffusion equations. More recent applications to heterogeneous problems can be found in [15,25].

We investigate now the scalability of the OSM for the one- and two-dimensional model problems introduced in Section 2. Like for the classical parallel Schwarz method, we show that the OSM is scalable for the solution of the two-dimensional problem, but not for the one-dimensional one, and we will also give some insight on the optimal choice for the Robin parameter.

4.1 Optimized Schwarz method in 1D

The error equations associated to the OSM for (2)-(3) are given by

$$\begin{aligned} \partial_{xx} e_j^n &= 0 \text{ in } (a_j,b_j),\\ \partial_x e_j^n(a_j) - p e_j^n(a_j) &= \partial_x e_{j-1}^{n-1}(a_j) - p e_{j-1}^{n-1}(a_j),\\ \partial_x e_j^n(b_j) + p e_j^n(b_j) &= \partial_x e_{j+1}^{n-1}(b_j) + p e_{j+1}^{n-1}(b_j), \end{aligned} \tag{15}$$

for $j = 2,\ldots,N-1$, where p is the Robin parameter, and

$$\begin{aligned} \partial_{xx} e_1^n &= 0 \text{ in } (a_1,b_1),\\ e_j^n(a_1) &= 0,\\ \partial_x e_1^n(b_1) + p e_1^n(b_1) &= \partial_x e_2^{n-1}(b_1) + p e_2^{n-1}(b_1), \end{aligned} \tag{16}$$

and

$$\begin{aligned} \partial_{xx} e_N^n &= 0 \text{ in } (a_N,b_N),\\ \partial_x e_N^n(a_N) - p e_N^n(a_N) &= \partial_x e_{N-1}^{n-1}(a_N) - p e_{N-1}^{n-1}(a_N),\\ e_N^n(b_N) &= 0. \end{aligned} \tag{17}$$

The corresponding solution in Ω_j is given by

$$e_j^n(x) = A_j^n x + B_j^n. \tag{18}$$

Defining

$$\begin{aligned} \mathscr{R}_-^{n-1}(a_j) &:= \partial_x e_{j-1}^{n-1}(a_j) - p e_{j-1}^{n-1}(a_j), \\ \mathscr{R}_+^{n-1}(b_j) &:= \partial_x e_{j+1}^{n-1}(b_j) + p e_{j+1}^{n-1}(b_j), \end{aligned} \tag{19}$$

and inserting (18) into the boundary conditions in (15), we get the linear system

$$\begin{aligned} A_j^n - pA_j^n a_j - pB_j &= \mathscr{R}_-^{n-1}(a_j), \\ A_j^n + pA_j^n b_j + pB_j &= \mathscr{R}_+^{n-1}(b_j), \end{aligned}$$

whose solution is

$$A_j^n = \frac{1}{\kappa} p\big(\mathscr{R}_-^{n-1}(a_j) + \mathscr{R}_+^{n-1}(b_j)\big),\ B_j^n = \frac{1}{\kappa}\big((1-pa_j)\mathscr{R}_+^{n-1}(b_j) - (1+pb_j)\mathscr{R}_-^{n-1}(a_j)\big),$$

with $\kappa := 2p + p^2(L+2\delta)$. Inserting A_j^n and B_j^n into (18) and using $b_j = a_j + L + 2\delta$, we get

$$\begin{aligned} e_j^n(x) = \frac{1}{\kappa}\Big[& p\left(\mathscr{R}_-^{n-1}(a_j) + \mathscr{R}_+^{n-1}(b_j)\right)x + \mathscr{R}_+^{n-1}(b_j) - \mathscr{R}_-^{n-1}(a_j) \\ & - pa_j\left(\mathscr{R}_-^{n-1}(a_j) + \mathscr{R}_+^{n-1}(b_j)\right) - p(L+2\delta)\mathscr{R}_-^{n-1}(a_j)\Big]. \end{aligned} \tag{20}$$

Now, we construct the iteration matrix of the OSM. To do so, we recall the definition (19) of $\mathscr{R}_-^n(a_j)$ and $\mathscr{R}_+^n(b_j)$ and insert (20) in to (19) to obtain, for $j = 2,\dots,N-1$, that

$$\begin{bmatrix} \mathscr{R}_-^n(a_j) \\ \mathscr{R}_+^n(b_j) \end{bmatrix} = T_1 \begin{bmatrix} \mathscr{R}_-^{n-1}(a_{j-1}) \\ \mathscr{R}_+^{n-1}(b_{j-1}) \end{bmatrix} + T_2 \begin{bmatrix} \mathscr{R}_-^{n-1}(a_{j+1}) \\ \mathscr{R}_+^{n-1}(b_{j+1}) \end{bmatrix},$$

where

$$T_1 := \frac{p}{\kappa}\begin{bmatrix} (2 - pL + p(L+2\delta)) & -pL \\ 0 & 0 \end{bmatrix}, \quad T_2 := \frac{p}{\kappa}\begin{bmatrix} 0 & 0 \\ 2p\delta - p(L+2\delta) & (2+2p\delta) \end{bmatrix}.$$

Similarly, for the subdomains Ω_1, Ω_2, Ω_{N-1}, and Ω_N we obtain

$$\begin{aligned} \begin{bmatrix} 0 \\ \mathscr{R}_+^n(b_1) \end{bmatrix} &= T_2 \begin{bmatrix} \mathscr{R}_-^{n-1}(a_2) \\ \mathscr{R}_+^{n-1}(b_2) \end{bmatrix}, \\ \begin{bmatrix} \mathscr{R}_-^n(a_2) \\ \mathscr{R}_+^n(b_2) \end{bmatrix} &= \widetilde{T}_1 \begin{bmatrix} 0 \\ \mathscr{R}_+^{n-1}(b_1) \end{bmatrix} + T_2 \begin{bmatrix} \mathscr{R}_-^{n-1}(a_3) \\ \mathscr{R}_+^{n-1}(b_3) \end{bmatrix}, \\ \begin{bmatrix} \mathscr{R}_-^n(a_{N-1}) \\ \mathscr{R}_+^n(b_{N-1}) \end{bmatrix} &= T_1 \begin{bmatrix} \mathscr{R}_-^{n-1}(a_{N-2}) \\ \mathscr{R}_+^{n-1}(b_{N-2}) \end{bmatrix} + \widetilde{T}_2 \begin{bmatrix} \mathscr{R}_-^{n-1}(a_n) \\ 0 \end{bmatrix}, \\ \begin{bmatrix} \mathscr{R}_-^n(a_N) \\ 0 \end{bmatrix} &= T_1 \begin{bmatrix} \mathscr{R}_-^{n-1}(a_{N-1}) \\ \mathscr{R}_+^{n-1}(b_{N-1}) \end{bmatrix}, \end{aligned}$$

where

$$\widetilde{T}_1 := \begin{bmatrix} 0 & \frac{1-pL}{(1+p(L+2\delta))} \\ 0 & 0 \end{bmatrix}, \quad \widetilde{T}_2 := \begin{bmatrix} 0 & 0 \\ \frac{1-pL}{(1+p(L+2\delta))} & 0 \end{bmatrix}.$$

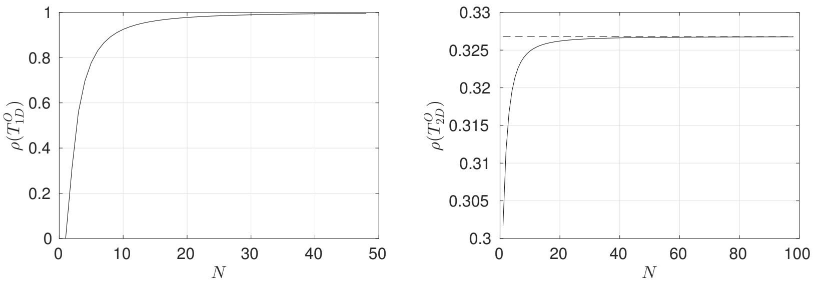

Fig. 5 Left: spectral radius of the iteration matrix T^O_{1D} corresponding to $L = 1$, $\delta = 0.1$. Right: comparison of the spectral radius (solid line) and infinity norm (dashed line) of the matrix T^O_{2D} corresponding to $L = 1$, $\widehat{L} = 1$, $\delta = 0.1$, $p = 1$, and $k = \pi$.

Introducing the vector

$$\begin{aligned}\mathbf{r}^n := \big[0\,, \mathscr{R}^n_+(b_1)\,, \mathscr{R}^n_-(a_2)\,, \mathscr{R}^n_+(b_2)\,, \cdots, \mathscr{R}^n_-(a_j)\,, \mathscr{R}^n_+(b_j)\,, \cdots,\\ \mathscr{R}^n_-(a_{N-1})\,, \mathscr{R}^n_+(b_{N-1})\,, \mathscr{R}^n_-(a_N)\,, 0\big]^\top,\end{aligned} \tag{21}$$

we get

$$\mathbf{r}^n = T^O_{1D}\mathbf{r}^{n-1},$$

where the iteration matrix T^O_{1D} is given by

$$T^O_{1D} := \begin{bmatrix} & T_2 & & & & & & \\ \widetilde{T}_1 & & T_2 & & & & & \\ & T_1 & & T_2 & & & & \\ & & T_1 & & T_2 & & & \\ & & & \ddots & & \ddots & & \\ & & & & T_1 & & T_2 & \\ & & & & & T_1 & & \widetilde{T}_2 \\ & & & & & & T_1 & \end{bmatrix}. \tag{22}$$

Like in Section 3.1, we compute numerically the spectral radius of T^O_{1D}. For given values of δ and p, $\rho(T^O_{1D})$ is depicted as a function of N in Figure 5 (left). It is clear that $\rho(T^O_{1D}) \to 1$ as N increases for any δ and p. This means that also the OSM for the solution of the one-dimensional problem is not scalable.

Next, we explain the observed bound $\rho(T^O_{1D}) \leq 1$ for any N. Exploiting the structure of T^O_{1D}, and recalling the definitions of T_1, T_2, $\widetilde{T}_1$, and $\widetilde{T}_2$, we obtain

$$\|T^O_{1D}\|_\infty = \max\left\{\frac{p}{\kappa}(|2-pL+p(L+2\delta)|+pL), \frac{p}{\kappa}(|2p\delta-p(L+2\delta)|+2+2p\delta), \frac{|1-pL|}{1+p(L+2\delta)}\right\}.$$

Studying the first two terms, with $\kappa := 2p + p^2(L+2\delta)$, we observe that

$$\begin{aligned}\frac{p}{\kappa}(|2-pL+p(L+2\delta)|+pL) &= \frac{1}{2+p(L+2\delta)}(2+p(L+2\delta)) = 1,\\ \frac{p}{\kappa}(|2p\delta-p(L+2\delta)|+2+2p\delta) &= \frac{1}{2+p(L+2\delta)}(2+2p\delta+pL) = 1.\end{aligned}$$

Moreover, it is evident that the third term is smaller than 1. Hence, we conclude that $\|T^O_{1D}\|_\infty = 1$, which explains the bound $\rho(T^O_{1D}) \leq 1$. The bound $\|T^O_{1D}\|_\infty = 1$ is shown in Figure 5 (left).

We now show that it is possible to make the one-dimensional OSM convergent in a finite number of iterations. To do so, we use a different Robin parameter p in (15) for each subdomain Ω_j, namely

$$\begin{aligned} \partial_{xx} e_j^n &= 0 \text{ in } (a_j, b_j), \\ \partial_x e_j^n(a_j) - p_j^- e_j^n(a_j) &= \partial_x e_{j-1}^{n-1}(a_j) - p_j^- e_{j-1}^{n-1}(a_j), \\ \partial_x e_j^n(b_j) + p_j^+ e_j^n(b_j) &= \partial_x e_{j+1}^{n-1}(b_j) + p_j^+ e_{j+1}^{n-1}(b_j), \end{aligned} \tag{23}$$

where $p_j^- > 0$ and $p_j^+ > 0$ are given by the following theorem, which is proved using similar arguments as in [5].

Theorem 2 *Let $L_j^+ := b_N - b_j, j = 1\ldots, N-1$, $L_j^- := a_j - a_1, j = 2, \ldots, N$. If we set $p_j^+ := 1/L_j^+, j = 1\ldots, N-1$, $p_j^- = 1/L_{j-1}^-, j = 2, \ldots, N$, then the OSM* (23) *converges exactly in N iterations.*

Proof First we prove that p_j^+, p_j^-, satisfy the following property:

$$\partial_x e_j^n + p_j^+ e_j^n = 0 \text{ on } x = b_j \quad \Longrightarrow \quad \partial_x e_j^n + p_{j-1}^+ e_j^n = 0 \text{ on } x = b_{j-1}, \tag{24}$$

$$\partial_x e_j^n - p_j^- e_j^n = 0 \text{ on } x = a_{j-1} \quad \Longrightarrow \quad \partial_x e_j^n - p_{j+1}^- e_j^n = 0 \text{ on } x = a_j. \tag{25}$$

To do so, suppose that $\partial_x e_j^n(b_j) + p_j^+ e_j^n(b_j) = 0$. Let v be defined on (b_{j-1}, b_N) by $v(x) := \frac{e_j^n(b_{j-1})}{L_{j-1}^+}(b_N - x)$, we have that $\partial_x v(b_j) + p_j^+ v(b_j) = 0$ and by construction $v(b_{j-1}) = e_j^n(b_{j-1})$. Hence v satisfies

$$\begin{aligned} -\partial_{xx}(e_j^n - v) &= 0 \text{ in } (b_{j-1}, b_j), \\ e_j^n - v &= 0 \text{ on } x = b_{j-1}, \\ (\partial_x + p_j^+)(e_j^n - v) &= 0 \text{ on } x = b_j. \end{aligned} \tag{26}$$

By uniqueness of the solution of (26) we have that $e_j^n = v$ on (b_{j-1}, b_j), and we conclude that $\partial_x e_j^n(b_{j-1}) + p_{j-1}^+ e_j^n(b_{j-1}) = 0$ since this holds for v. Similarly, suppose that $\partial_x e_j^n(a_{j-1}) - p_j^- e_j^n(a_{j-1}) = 0$, and let w be defined on (a_0, a_j) by $w(x) = \frac{e_j^n(x_j)}{L_j^-}(x - a_0)$. It holds that $\partial_x w(a_{j-1}) - p_j^- w(a_{j-1}) = 0$ and $w(a_j) = e_j^n(a_j)$. Hence w verifies

$$\begin{aligned} \partial_{xx}(e_j^n - w) &= 0 \text{ in } (a_{j-1}, a_j), \\ (\partial_x - p_j^-)(e_j^n - w) &= 0 \text{ on } x = a_{j-1}, \\ e_j^n - w &= 0 \text{ on } x = a_j, \end{aligned}$$

which implies that $e_j^n = w$. Therefore $\partial_x e_j^n(a_j) - p_{j+1}^- e_j^n(a_j) = 0$.

Now we prove that the OSM (23) converges in N iterations. A direct calculation shows that the choices $p_2^- = \frac{1}{L_1^-}$ and $p_{N-1}^+ = \frac{1}{L_{N-1}^+}$ imply that $\partial_x e_1^n(a_1) - p_2^- e_n^1(a_1) = 0$ and $\partial_x e_N^n(b_{N-1}) + p_{N-1}^+ e_N^n(b_{N-1}) = 0$ for any $n \geq 0$. Hence, the transmission conditions in (23) allow us to write

$$\begin{aligned} \partial_x e_2^{n+1}(a_1) - p_2^- e_2^{n+1}(a_1) &= \partial_x e_1^n(a_1) - p_2^- e_1^n(a_1) = 0, \\ \partial_x e_{N-1}^{n+1}(b_{N-1}) + p_{N-1}^+ e_{N-1}^{n+1}(b_{N-1}) &= \partial_x e_N^n(b_{N-1}) + p_{N-1}^+ e_N^n(b_{N-1}) = 0, \end{aligned}$$

for any $n \geq 0$. Using (24) and (25) and again the transmission conditions in (23), we get

$$\partial_x e_3^{n+1}(a_2) - p_3^- e_3^{n+1}(a_2) = \partial_x e_2^n(a_2) - p_3^- e_2^n(a_2) = 0,$$
$$\partial_x e_{N-2}^{n+1}(b_{N-2}) + p_{N-2}^+ e_{N-2}^{n+1}(b_{N-2}) = \partial_x e_{N-1}^n(b_{N-2}) + p_{N-2}^+ e_{N-1}^n(b_{N-2}) = 0,$$

for $n \geq 1$. By induction, we obtain that after N iterations that the errors e_j^N satisfy

$$\begin{aligned} -\partial_{xx} e_j^N &= 0 \text{ in } (a_j, b_j), \\ (\partial_x + p_j^+) e_j^N &= 0 \text{ on } x = b_j, \\ (\partial_x - p_j^-) e_j^N &= 0 \text{ on } x = a_j, \end{aligned}$$

and

$$\begin{aligned} -\partial_{xx} e_1^N &= 0 \text{ in } (a_1, b_1), & -\partial_{xx} e_N^N &= 0 \text{ in } (a_N, b_N), \\ e_1^N &= 0 \text{ on } x = a_1, & (\partial_x - p_N^-) e_N^N &= 0 \text{ on } x = a_N, \\ (\partial_x + p_1^+) e_1^N &= 0 \text{ on } x = b_1, & e_N^N &= 0 \text{ on } x = b_N. \end{aligned}$$

Hence $e_j^N = 0$, for $j = 1 \dots, N$, which concludes our proof.

The one-dimensional result above can be generalized to higher dimensions by replacing the parameter p with a suitably chosen global operator (in general a Dirichlet-to-Neumann operator), see [36]. This choice is computationally expensive in practice, and hence the global operator is often approximated by local operators [28].

4.2 Optimized Schwarz method in 2D

Let us consider problem (4)-(5). The OSM (in error form) is given by

$$\begin{aligned} -\Delta e_j^n &= 0 \text{ in } \Omega_j, \\ e_j^n(\cdot, 0) &= 0,\ e_j^n(\cdot, \widehat{L}) = 0, \\ \partial_x e_j^n(a_j, \cdot) - p e_j^n(a_j, \cdot) &= \partial_x e_{j-1}^{n-1}(a_j, \cdot) - p e_{j-1}^{n-1}(a_j, \cdot), \\ \partial_x e_j^n(b_j, \cdot) + p e_j^n(b_j, \cdot) &= \partial_x e_{j+1}^{n-1}(b_j, \cdot) + p e_{j+1}^{n-1}(b_j, \cdot), \end{aligned} \tag{27}$$

for $j = 2, \dots, N-1$, and

$$\begin{aligned} -\Delta e_1^n &= 0 \quad \text{in } \Omega_1, & -\Delta e_N^n &= 0 \text{ in } \Omega_N, \\ e_1^n(\cdot, 0) &= 0,\ e_1^n(\cdot, \widehat{L}) = 0, & e_N^n(\cdot, 0) &= 0,\ e_N^n(\cdot, \widehat{L}) = 0, \\ e_1^n(a_1, \cdot) &= 0, & (\partial_x - p) e_N^n(a_N, \cdot) &= (\partial_x - p) e_{N-1}^{n-1}(a_N, \cdot), \\ (\partial_x + p) e_1^n(b_1, \cdot) &= (\partial_x + p) e_2^{n-1}(b_1, \cdot), & e_N^n(b_N, \cdot) &= 0. \end{aligned}$$

As in Section 3.2, we use the Fourier expansion $e_j^n(x,y) = \sum_{m=1}^{\infty} v_j^n(x,k) \sin(ky)$ with $k = \frac{\pi m}{\widehat{L}}$. The Fourier coefficients v_j^n must satisfy

$$\begin{aligned} \partial_{xx} v_j^n &= k^2 v_j^n \text{ in } (a_j, b_j), \\ \partial_x v_j^n(a_j) - p v_j^n(a_j) &= \partial_x v_{j-1}^{n-1}(a_j) - p v_{j-1}^{n-1}(a_j), \\ \partial_x v_j^n(b_j) + p v_j^n(b_j) &= \partial_x v_{j+1}^{n-1}(b_j) + p v_{j+1}^{n-1}(b_j). \end{aligned} \tag{28}$$

Defining $\mathscr{R}_-^{n-1}(a_j) := \partial_x v_{j-1}^{n-1}(a_j) - p v_{j-1}^{n-1}(a_j)$ and $\mathscr{R}_+^{n-1}(b_j) := \partial_x v_{j+1}^{n-1}(b_j) + p v_{j+1}^{n-1}(b_j)$, the solution to (28) is given by

$$\begin{aligned} v_j^n(x,k) = \mathscr{R}_-^{n-1}(a_j)&\left[-\frac{1}{\gamma}(k-p)e^{k(x-b_j)} - \frac{1}{\gamma}(k+p)e^{k(b_j-x)}\right] \\ +\mathscr{R}_+^{n-1}(b_j)&\left[\frac{1}{\gamma}(k+p)e^{k(x-a_j)} + \frac{1}{\gamma}(k-p)e^{k(a_j-x)}\right], \end{aligned} \tag{29}$$

where $\gamma := (k+p)^2 e^{k(L+2\delta)} - (k-p)^2 e^{-k(L+2\delta)}$. As for the 1D case, we insert (29) into the definitions of $\mathscr{R}_-^n(a_j)$ and $\mathscr{R}_+^n(b_j)$ to get

$$\begin{bmatrix} \mathscr{R}_-^n(a_j) \\ \mathscr{R}_+^n(b_j) \end{bmatrix} = T_1 \begin{bmatrix} \mathscr{R}_-^{n-1}(a_{j-1}) \\ \mathscr{R}_+^{n-1}(b_{j-1}) \end{bmatrix} + T_2 \begin{bmatrix} \mathscr{R}_-^{n-1}(a_{j+1}) \\ \mathscr{R}_+^{n-1}(b_{j+1}) \end{bmatrix}, \tag{30}$$

where

$$T_1 := \begin{bmatrix} g_3 - pg_1 & g_4 - pg_2 \\ 0 & 0 \end{bmatrix}, \qquad T_2 := \begin{bmatrix} 0 & 0 \\ g_4 - pg_2 & g_3 - pg_1 \end{bmatrix},$$

with

$$\begin{aligned} g_1 &:= -\frac{1}{\gamma}(k-p)e^{-2\delta k} - \frac{1}{\gamma}(k+p)e^{2\delta k}, \qquad g_2 := \frac{1}{\gamma}(k+p)e^{kL} + \frac{1}{\gamma}(k-p)e^{-kL}, \\ g_3 &:= \frac{-k}{\gamma}(k-p)e^{-2\delta k} + \frac{k}{\gamma}(k+p)e^{2\delta k}, \quad g_4 := \frac{k}{\gamma}(k+p)e^{kL} - \frac{k}{\gamma}(k-p)e^{-kL}. \end{aligned} \tag{31}$$

Similar arguments allow us to obtain for the subdomains Ω_1, Ω_2, Ω_{N-1}, and Ω_N the relations

$$\begin{aligned} \begin{bmatrix} 0 \\ \mathscr{R}_+^n(b_1) \end{bmatrix} &= T_2 \begin{bmatrix} \mathscr{R}_-^{n-1}(a_2) \\ \mathscr{R}_+^{n-1}(b_2) \end{bmatrix}, \\ \begin{bmatrix} \mathscr{R}_-^n(a_2) \\ \mathscr{R}_+^n(b_2) \end{bmatrix} &= \widetilde{T}_1 \begin{bmatrix} 0 \\ \mathscr{R}_+^{n-1}(b_1) \end{bmatrix} + T_2 \begin{bmatrix} \mathscr{R}_-^{n-1}(a_3) \\ \mathscr{R}_+^{n-1}(b_3) \end{bmatrix}, \\ \begin{bmatrix} \mathscr{R}_-^n(a_{N-1}) \\ \mathscr{R}_+^n(b_{N-1}) \end{bmatrix} &= T_1 \begin{bmatrix} \mathscr{R}_-^{n-1}(a_{N-2}) \\ \mathscr{R}_+^{n-1}(b_{N-2}) \end{bmatrix} + \widetilde{T}_2 \begin{bmatrix} \mathscr{R}_-^{n-1}(a_n) \\ 0 \end{bmatrix}, \\ \begin{bmatrix} \mathscr{R}_-^n(a_N) \\ 0 \end{bmatrix} &= T_1 \begin{bmatrix} \mathscr{R}_-^{n-1}(a_{N-1}) \\ \mathscr{R}_+^{n-1}(b_{N-1}) \end{bmatrix}, \end{aligned} \tag{32}$$

where

$$\widetilde{T}_1 := \begin{bmatrix} 0 & \frac{(k+p)e^{-kL}+(k-p)e^{kL}}{(k+p)e^{k(L+2\delta)}+(k-p)e^{-k(L+2\delta)}} \\ 0 & 0 \end{bmatrix}, \quad \widetilde{T}_2 := \begin{bmatrix} 0 & 0 \\ \frac{(k+p)e^{-kL}+(k-p)e^{kL}}{(k+p)e^{k(L+2\delta)}+(k-p)e^{-k(L+2\delta)}} & 0 \end{bmatrix}.$$

Similarly as in Section 4.1 we use (30)-(32) to construct the iteration relation $\mathbf{r}^n = T_{2D}^O \mathbf{r}^{n-1}$, where T_{2D}^O is a block matrix with the same structure as in (22). We are now ready to prove scalability of the OSM in the overlapping case:

Theorem 3 *Recall* (31) *and define* $\varphi(k,\delta,p) := |g_3 - pg_1| + |g_4 - pg_2|$. *The OSM with overlap,* $\delta > 0$*, for the solution of problem* (27) *is scalable, in the sense that* $\rho(T_{2D}^O(k,\delta,p)) \leq \|T_{2D}^O(k,\delta,p)\|_\infty \leq \max_k \max\{\varphi(k,\delta,p), \|\widetilde{T}_1(k,\delta,p)\|_\infty\} < 1$ *(independently of N) for every* $p \geq 0$.

Proof Because of the structure of T_{2D}^O (as in (22)), the norm $\|T_{2D}^O\|_\infty$ is given by

$$\|T_{2D}^O\|_\infty = \max_i \sum_j |(T_{2D}^O)_{i,j}| = \max\{\,\varphi(k,\delta,p)\,,\,\|\widetilde{T}_1\|_\infty\,,\,\|\widetilde{T}_2\|_\infty\,\}.$$

We begin by showing that $\varphi(k,\delta,p) < 1$ for any $k,p \in [0,\infty)$ and $\delta > 0$. To do so, we notice that

$$\begin{aligned}|g_3 - pg_1| &= |\frac{1}{\gamma}(-k(k-p)e^{-2\delta k} + k(k+p)e^{2\delta k} + p(k-p)e^{-2\delta k} + p(k+p)e^{2\delta k})| \\ &= \frac{1}{\gamma}|(k+p)^2 e^{2\delta k} - (k-p)^2 e^{-2\delta k})| = \frac{1}{\gamma}((k+p)^2 e^{2\delta k} - (k-p)^2 e^{-2\delta k})\end{aligned}$$

and

$$\begin{aligned}|g_4 - pg_2| &= \frac{1}{\gamma}|(k(k-p)e^{kL} - k(k-p)e^{-kL} - p(k+p)e^{kL} - p(k-p)e^{-kL})| \\ &= \frac{1}{\gamma}(k+p)|k-p|(e^{kL} - e^{-kL}),\end{aligned}$$

which implies that

$$\varphi(k,\delta,p) = \frac{(k+p)^2 e^{2\delta k} - (k-p)^2 e^{-2\delta k} + (k+p)|k-p|(e^{kL} - e^{-kL})}{(k+p)^2 e^{kL+2k\delta} - (k-p)^2 e^{-kL-2k\delta}}.$$

By computing the derivative of φ with respect to p we find

$$\begin{aligned}\frac{\partial\varphi}{\partial p} &= -\frac{2ke^{2\delta k+2kL} - 2ke^{2\delta k}}{k^2 e^{4\delta k} + 2ke^{4\delta k} + p^2 e^{4\delta k} e^{2kL} + 2k^2 e^{2\delta k} - 2e^{2\delta k} p^2 e^{kL} + (p-k)^2} \quad \text{for } p<k, \\ \frac{\partial\varphi}{\partial p} &= \frac{2ke^{2\delta k+2kL} - 2ke^{2\delta k}}{k^2 e^{4\delta k} + 2ke^{4\delta k} + p^2 e^{4\delta k} e^{2kL} + 2p^2 e^{2\delta k} - 2e^{2\delta k} k^2 e^{kL} + (k-p)^2} \quad \text{for } p>k.\end{aligned}$$

Analyzing the signs of these derivatives, we see that $\varphi(k,\delta,p)$ is strictly decreasing for $p < k$ and it is strictly increasing for $p > k$, thus it reaches a minimum for $p = k$. Therefore the maximum of $\varphi(k,\delta,p)$ with respect to the variable p is obtained for $p = 0$ and for $p \to +\infty$:

$$\varphi(k,\delta,p) \le \max\Big\{\,\varphi(k,\delta,0)\,,\,\lim_{p\to\infty}\varphi(k,\delta,p)\,\Big\}.$$

For $p = 0$, $\delta > 0$ and $L > 0$ we have

$$\begin{aligned}\varphi(k,\delta,p) &= \frac{e^{2\delta k} - e^{-2\delta k} + e^{kL} - e^{-kL}}{e^{kL+2\delta k} - e^{-kL-2\delta k}} \\ &= \frac{\sinh(2\delta k) + \sinh(kL)}{\sinh(kL)\cosh(2\delta k) + \sinh(2\delta k)\cosh(kL)} < 1,\end{aligned}$$

and, under the same conditions,

$$\lim_{p\to\infty}\varphi(k,\delta,p) = \frac{\sinh(2\delta k) + \sinh(kL)}{\sinh(kL)\cosh(2\delta k) + \sinh(2\delta k)\cosh(kL)} = \varphi(k,\delta,0) < 1.$$

Hence, it holds that $\varphi(k,\delta,p) \le \varphi(k,\delta,0) < 1$. We now focus on $\|\widetilde{T}_1\|_\infty$ and $\|\widetilde{T}_2\|_\infty$. Notice that $\|\widetilde{T}_1\|_\infty = \|\widetilde{T}_2\|_\infty$ and

$$\|\widetilde{T}_1\|_\infty = \left|\frac{(k+p)e^{-kL}+(k-p)e^{kL}}{(k+p)e^{k(L+2\delta)}+(k-p)e^{-k(L+2\delta)}}\right| = \left|\frac{k\cosh(kL)-p\sinh(kL)}{k\cosh(k(L+2\delta))+p\sinh(k(L+2\delta))}\right| < 1.$$

In order to get a bound independently of k, we observe that $\lim_{k\to\infty}\varphi(k,\delta,p) = \lim_{k\to\infty}\|\widetilde{T}_1\|_\infty = 0$ if $\delta > 0$. Therefore defining $\bar{\rho}(\delta) := \max_k \max\{\varphi(k,\delta,p), \|\widetilde{T}_1(k,\delta,p)\|_\infty\}$, we see that $\|T_{2D}^O\|_\infty = \max\{\varphi, \|\widetilde{T}_1\|, \|\widetilde{T}_2\|\} < \bar{\rho}(\delta) < 1$, for every $k,\delta,p > 0$.

Figure 5 (right) shows the behavior of the infinity norm and of the spectral radius of T_{2D}^O for a given value of p.

For the case without overlap, we need a further argument because for $\delta = 0$ both $\rho(T_{2D}^O)$ and $\|T_{2D}^O\|_\infty$ are less then one for any finite frequency k, but tend to one as $k \to \infty$. One can therefore construct a situation where the method would not be scalable as follows: suppose we have N subdomains, and on the j-th subdomain we choose for the initial guess e_j^0 the j-th frequency $e_j^0 = \hat{e}_j^0 \sin(j\frac{\pi}{L}y)$. Then the convergence of the method is determined by the frequency which maximizes $\rho(T_{2D}^O(k))$. When the number of subdomains N becomes large, this maximum is attained for the largest frequency $k_N = N\frac{\pi}{Ly}$ since $\rho(T_{2D}^O(k)) \to 1$ as $k \to \infty$. Thus, every time we add a subdomain to the chain with a new initial condition on the interface $N+1$ according to our rule, the convergence rate of the method deteriorates from $\rho(T_{2D}^O(N\frac{\pi}{L}))$ to $\rho(T_{2D}^O((N+1)\frac{\pi}{L}))$ and the scalability property is lost. Theorem 4 gives however a sufficient condition such that the OSM is weakly scalable also without overlap, and to see this we introduce the vector $\mathbf{e}^n$ with $e_k^n = \|\mathbf{r}^n(k)\|_\infty$ where $\mathbf{r}^n(k)$, defined in (21), contains the Robin traces at the interfaces of the k-th Fourier mode.

Theorem 4 *Given a tolerance* `Tol`*, and supposing there exists a* $\tilde{k}$ *that does not depend on* N *such that* $e_k^0 <$ `Tol` *for every* $k > \tilde{k}$*, then the OSM without overlap,* $\delta = 0$*, and* $p > 0$ *is weakly scalable.*

Proof Suppose that the initial guess satisfies $\|\mathbf{e}^0\|_\infty >$ `Tol`, since otherwise there is nothing to prove. Then, due to the hypothesis, we have that $\max_{\frac{\pi}{L}\le k\le\tilde{k}} e_k^0 >$ `Tol`. We now show that the method contracts with a ρ independent of the number of subdomains up to the tolerance `Tol`, and therefore we have scalability. Indeed, for every k such that $\frac{\pi}{L} \le k \le \tilde{k}$

$$e_k^n = \|\mathbf{r}^n(k)\|_\infty \le \|T_{2D}^O(k)\|_\infty \|\mathbf{r}^{n-1}(k)\|_\infty \le \|T_{2D}^O(\bar{k})\|_\infty \|\mathbf{r}^{n-1}(k)\|_\infty = \|T_{2D}^O(\bar{k})\|_\infty e_k^{n-1},$$

where $\|T_{2D}^O(\bar{k})\|_\infty = \max_{\frac{\pi}{L}\le k\le\tilde{k}} \|T_{2D}^O(k)\|_\infty < 1$ because $\|T_{2D}^O(k)\|_\infty$ is strictly less then 1 for every finite k. Now for $k > \tilde{k}$,

$$e_k^n = \|\mathbf{r}^n(k)\|_\infty \le \|T_{2D}^O(k)\|_\infty \|\mathbf{r}^{n-1}(k)\|_\infty \le \|\mathbf{r}^{n-1}(k)\|_\infty = e_k^{n-1},$$

since $\|T_{2D}^O(k)\|_\infty \le 1$. Therefore we observe that the method does not increase the error for the frequencies $k > \tilde{k}$ while it contracts for the other frequencies with a contraction factor of at least $\bar{\rho} = \|T_{2D}^O(\bar{k})\|_\infty < 1$. Hence, as long as $\|\mathbf{e}^n\|_\infty >$ `Tol`, we have $\|\mathbf{e}^n\|_\infty \le \bar{\rho}^n \|\mathbf{e}^0\|_\infty$ with $\bar{\rho}$ independent of N.

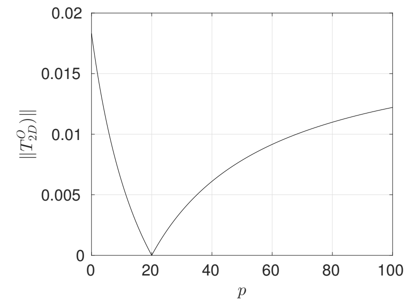

Fig. 6 Infinity norm of the iteration matrix T_{2D}^{O} as a function of p for $L = 1, \widehat{L} = 1, \delta = 0.1, k = 20, N = 50$.

Note that the technical assumption in Theorem 4 on the frequency content of the initial error is not restrictive, since in a numerical implementation we have a maximum frequency $k_{\max}$ which can be represented by the grid. Choosing $\tilde{k} = k_{\max}$, the hypothesis of Theorem 4 is verified.

Note also that without overlap, $\delta = 0$, we have that $\|T_{2D}^{O}\|_\infty = 1$ for $p = 0$ or $p \to \infty$. Therefore we can not conclude that the method is scalable in these two cases. For $p = 0$, the OSM exchanges only partial derivatives information on the interface. For $p \to \infty$, we obtain the classical Schwarz algorithm and it is well known [14] that without overlap ($\delta = 0$), the method does not converge.

We finally show the behavior of $p \mapsto \|T_{2D}^{O}(k,\delta,p)\|_\infty$ for a fixed pair (δ,k) in Figure 6. According to the proof of Theorem 3, the minimum of the function $p \mapsto \varphi(k,\delta,p)$ is located at $p = k$. Even though it is a minimum for $\varphi(k,\delta,p)$ and not necessarily for $\|T_{2D}^{O}(k,\delta,p)\|_\infty$ or $\rho(T_{2D}^{O})$, we might deduce from Figure 6 that in order to eliminate the k-th frequency, a good choice would be to set $p := k$ in the OSM. For the Laplace equation, it has been shown for two subdomains that setting $p := k$ leads to a vanishing convergence factor $\rho(k)$ for the frequency k. In the case of many subdomains, a similar result has not been proved yet, but Figure 6 indicates that it might hold as well.

5 Dirichlet-Neumann method

In this section, we study a parallel Dirichlet-Neumann method (PDNM) which, to the best of our knowledge, has not been studied in the literature for a chain of N fixed-sized subdomains. A discussion of this method for two subdomains is given in [2], see also [38] and [13, page 717]. We now show that as for the Schwarz methods, the PDNM in 1D is not scalable, while in 2D it is.

5.1 Dirichlet-Neumann method in 1D

Let us consider a set of domains $\Omega_j = (a_{j-1}, a_j)$, where $a_j = jL$. The subdomains have length L and do not overlap. Such a non-overlapping decomposition of Ω is shown in Figure 7, and corresponds to Figure 1 with $\delta = 0$ and $\overline{\Omega} = \cup_{j=1}^{N} \overline{\Omega}_j$. The error equations for PDNM

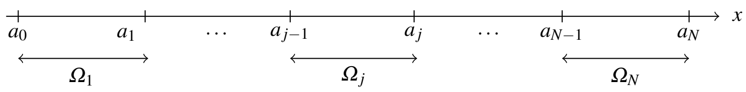

Fig. 7 One-dimensional chain of N non-overlapping fixed-sized subdomains.

are given by

$$\begin{aligned}\partial_{xx} e_j^n &= 0 \text{ in } (a_{j-1}, a_j),\\ e_j^n(a_j) &= (1-\theta) e_j^{n-1}(a_j) + \theta e_{j+1}^{n-1}(a_j),\\ \partial_x e_j^n(a_{j-1}) &= (1-\lambda)\partial_x e_j^{n-1}(a_{j-1}) + \mu \partial_x e_{j-1}^{n-1}(a_{j-1}),\end{aligned} \tag{33}$$

for $j = 2, \ldots, N-1$, and

$$\begin{aligned}\partial_{xx} e_1^n &= 0 \text{ in } (a_1, a_1),\\ e_1^n(a_0) &= 0,\\ e_1^n(a_1) &= (1-\theta) e_1^{n-1}(a_1) + \theta e_2^{n-1}(a_1),\end{aligned} \tag{34}$$

and

$$\begin{aligned}\partial_{xx} e_N^n &= 0 \text{ in } (a_{N-1}, a_N),\\ \partial_x e_N^n(a_{N-1}) &= (1-\mu)\partial_x e_N^{n-1}(a_{N-1}) + \mu \partial_x e_{N-1}^{n-1}(a_{N-1}),\\ e_N^n(a_N) &= 0.\end{aligned} \tag{35}$$

In (33)-(34), θ and μ are relaxation parameters in $(0,1)$. Now, we define

$$\mathscr{D}_j^n := e_j^n(a_j), \quad \mathscr{N}_j^n := \partial_x e_j^n(a_{j-1}),$$

and by a direct calculation we find that the solution to (33) is given by

$$e_j^n(x) = \mathscr{N}_j^n (x - a_j) + \mathscr{D}_j^n,$$

for $j = 2, \ldots, N-1$, and

$$e_1^n(x) = \frac{\mathscr{D}_1^n}{L}(x - a_0), \quad e_N^n(x) = \mathscr{N}_N^n (x - a_N).$$

Introducing these expressions into the transmission conditions in (33), we get

$$\begin{aligned}
\begin{bmatrix} 0 \\ \mathscr{D}_1^n \end{bmatrix} &= \widehat{T}_1 \begin{bmatrix} \mathscr{N}_1^{n-1} \\ \mathscr{D}_1^{n-1} \end{bmatrix} + T_2 \begin{bmatrix} \mathscr{N}_2^{n-1} \\ \mathscr{D}_2^{n-1} \end{bmatrix},\\
\begin{bmatrix} \mathscr{N}_2^n \\ \mathscr{D}_2^n \end{bmatrix} &= \widetilde{T}_0 \begin{bmatrix} 0 \\ \mathscr{D}_1^{n-1} \end{bmatrix} + T_1 \begin{bmatrix} \mathscr{N}_2^{n-1} \\ \mathscr{D}_2^{n-1} \end{bmatrix} + T_2 \begin{bmatrix} \mathscr{N}_3^{n-1} \\ \mathscr{D}_3^{n-1} \end{bmatrix},\\
\begin{bmatrix} \mathscr{N}_j^n \\ \mathscr{D}_j^n \end{bmatrix} &= T_0 \begin{bmatrix} \mathscr{N}_{j-1}^{n-1} \\ \mathscr{D}_{j-1}^{n-1} \end{bmatrix} + T_1 \begin{bmatrix} \mathscr{N}_j^{n-1} \\ \mathscr{D}_j^{n-1} \end{bmatrix} + T_2 \begin{bmatrix} \mathscr{N}_{j+1}^{n-1} \\ \mathscr{D}_{j+1}^{n-1} \end{bmatrix}, \text{ for } j = 3, \ldots, N-2,\\
\begin{bmatrix} \mathscr{N}_{N-1}^n \\ \mathscr{D}_{N-1}^n \end{bmatrix} &= T_0 \begin{bmatrix} \mathscr{N}_{N-2}^{n-1} \\ \mathscr{D}_{N-2}^{n-1} \end{bmatrix} + T_1 \begin{bmatrix} \mathscr{N}_{N-1}^{n-1} \\ \mathscr{D}_{N-1}^{n-1} \end{bmatrix} + \widetilde{T}_2 \begin{bmatrix} \mathscr{N}_N^{n-1} \\ 0 \end{bmatrix},\\
\begin{bmatrix} \mathscr{N}_N^n \\ 0 \end{bmatrix} &= \widetilde{T}_1 \begin{bmatrix} \mathscr{N}_N^{n-1} \\ \mathscr{D}_N^{n-1} \end{bmatrix} + \widetilde{T}_2 \begin{bmatrix} \mathscr{N}_{N-1}^{n-1} \\ \mathscr{D}_{N-1}^{n-1} \end{bmatrix},
\end{aligned} \tag{36}$$

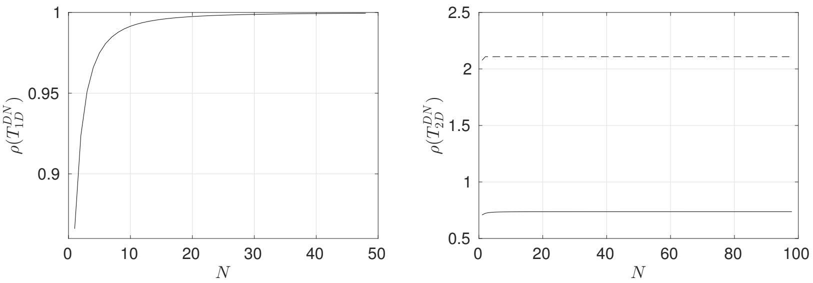

Fig. 8 Left: spectral radius of the iteration matrix T_{1D}^{DN} corresponding to $\theta = \mu = \frac{1}{2}$ and $L = 1$. Right: spectral radius (solid line) and infinity norm (dashed line) of the iteration matrix T_{2D}^{DN} corresponding to $\theta = \mu = \frac{1}{2}$, $L = 1$, $\widehat{L} = 1$, and $k = \pi$.

where

$$T_0 := \begin{bmatrix} \mu & 0 \\ 0 & 0 \end{bmatrix}, \quad T_1 := \begin{bmatrix} 1-\mu & 0 \\ 0 & 1-\theta \end{bmatrix}, \quad T_2 := \begin{bmatrix} 0 & 0 \\ -\theta L & \theta \end{bmatrix},$$
$$\widetilde{T}_0 := \begin{bmatrix} 0 & \frac{\mu}{L} \\ 0 & 0 \end{bmatrix}, \quad \widehat{T}_1 := \begin{bmatrix} 0 & 0 \\ 0 & 1-\theta \end{bmatrix}, \quad \widetilde{T}_1 := \begin{bmatrix} 1-\mu & 0 \\ 0 & 0 \end{bmatrix}, \quad \widetilde{T}_2 := \begin{bmatrix} 0 & 0 \\ -\theta L & 0 \end{bmatrix}.$$

Now, we define the vector

$$\mathbf{e}^n := \left[0, \mathscr{D}_1^n, \mathscr{N}_2^n, \mathscr{D}_2^n, \ldots, \mathscr{N}_j^n, \mathscr{D}_j^n, \ldots, \mathscr{N}_{N-1}^n, \mathscr{D}_{N-1}^n, \mathscr{N}_N^n, 0\right]^\top,$$

and write equations (36) in the compact form

$$\mathbf{e}^n = T_{1D}^{DN} \mathbf{e}^{n-1},$$

where T_{1D}^{DN} is the 1D iteration matrix defined by

$$T_{1D}^{DN} := \begin{bmatrix} \widehat{T}_1 & T_2 & & & & & & \\ \widetilde{T}_0 & T_1 & T_2 & & & & & \\ & T_0 & T_1 & T_2 & & & & \\ & & T_0 & T_1 & T_2 & & & \\ & & & \ddots & \ddots & \ddots & & \\ & & & & T_0 & T_1 & T_2 & \\ & & & & & T_0 & T_1 & \widetilde{T}_2 \\ & & & & & & T_0 & \widetilde{T}_1 \end{bmatrix}. \tag{37}$$

A numerical evaluation of the spectral radius of T_{1D}^{DN} (see, e.g., Figure 8) shows that the PDNM is not weakly scalable, since $\rho(T_{1D}^{DN}) \to 1$ for growing N, like for the Schwarz methods. Note however that, in contrast to what we have shown in Theorem 2 for the OSM, for $N > 2$ it is not possible in general to make the PDNM converge in a finite number of iterations, a fact that was proved for an alternating variant in [5, Proposition 5].

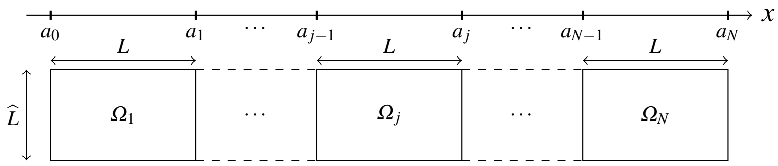

Fig. 9 Non overlapping domain decomposition in two dimensions. Notice that $a_j = jL$.

5.2 Dirichlet-Neumann method in 2D

We consider now the two dimensional problem whose non-overlapping domain decomposition is shown in Figure 9, which corresponds to Figure 2 with $\delta = 0$. The PDNM is given by

$$
\begin{aligned}
-\Delta e_j^n &= 0 \quad \text{in } \Omega_j,\\
e_j^n(\cdot,0) &= 0,\ e_j^n(\cdot,\widehat{L}) = 0,\\
e_j^n(a_j,\cdot) &= (1-\theta)e_j^{n-1}(a_j,\cdot) + \theta e_{j+1}^{n-1}(a_j,\cdot),\\
\partial_x e_j^n(a_{j-1},\cdot) &= (1-\mu)\partial_x e_j^{n-1}(a_{j-1},\cdot) + \mu\partial_x e_{j-1}^{n-1}(a_{j-1},\cdot),
\end{aligned}
$$

for $j = 2,\dots,N-1$, and

$$
\begin{aligned}
-\Delta e_1^n &= 0 \quad \text{in } \Omega_1,\\
e_1^n(\cdot,0) &= 0,\ e_1^n(\cdot,\widehat{L}) = 0,\\
e_1^n(a_0,\cdot) &= 0,\\
e_1^n(a_1,\cdot) &= (1-\theta)e_1^{n-1}(a_1,\cdot) + \theta e_2^{n-1}(a_1,\cdot),
\end{aligned}
$$

and

$$
\begin{aligned}
-\Delta e_N^n &= 0 \quad \text{in } \Omega_N,\\
e_N^n(\cdot,0) &= 0,\ e_N^n(\cdot,\widehat{L}) = 0,\\
\partial_x e_N^n(a_{N-1},\cdot) &= (1-\mu)\partial_x e_N^{n-1}(a_{N-1},\cdot) + \mu\partial_x e_{N-1}^{n-1}(a_{N-1},\cdot),\\
e_N^n(a_N,\cdot) &= 0,
\end{aligned}
$$

where $\theta,\mu \in (0,1)$. Now, we consider the Fourier expansion of e_j^n as in the previous sections. Since the Fourier coefficients $v_j^n(x,k)$ solve

$$
\begin{aligned}
\partial_{xx} v_j^n &= k^2 v_j^n \text{ in } (a_j,b_j),\\
v_j^n(a_j) &= (1-\theta)v_j^{n-1}(a_j) + \theta v_{j+1}^{n-1}(a_j),\\
\partial_x v_j^n(a_{j-1}) &= (1-\mu)\partial_x v_j^{n-1}(a_{j-1}) + \mu\partial_x v_{j-1}^{n-1}(a_{j-1}),
\end{aligned}
$$

defining

$$
\begin{aligned}
\mathscr{D}_j^n &:= (1-\theta)v_j^{n-1}(a_j) + \theta v_{j+1}^{n-1}(a_j),\\
\mathscr{N}_j^n &:= (1-\mu)\partial_x v_j^{n-1}(a_{j-1}) + \mu\partial_x v_{j-1}^{n-1}(a_{j-1}),
\end{aligned}
$$

we get

$$v_j^n(x,k) = \frac{1}{k\gamma_2}\left[ke^{-k[(j-1)L-x]}\mathscr{D}_j^n + e^{-k(jL-x)}\mathscr{N}_j^n + ke^{k[(j-1)L-x]}\mathscr{D}_j^n - e^{k(jL-x)}\mathscr{N}_j^n\right],$$

for $j = 2,\dots,N-1$, and

$$v_1^n(x,k) = \frac{D_1^n}{\gamma_1}[e^{kx} - e^{-kx}], \quad v_N^n(x,k) = \frac{1}{k\gamma_2}\left[e^{-k(NL-x)}N_N^n - e^{k(NL-x)}N_N^n\right],$$

where $\gamma_1 := e^{-kL} - e^{kL}$ and $\gamma_2 := e^{kL} + e^{-kL}$. Exploiting the definition of $\mathscr{N}_j^n$ and $\mathscr{D}_j^n$, we get

$$\begin{aligned}
\begin{bmatrix} 0 \\ \mathscr{D}_1^n \end{bmatrix} &= \widehat{T}_1 \begin{bmatrix} \mathscr{N}_1^{n-1} \\ \mathscr{D}_1^{n-1} \end{bmatrix} + T_2 \begin{bmatrix} \mathscr{N}_2^{n-1} \\ \mathscr{D}_2^{n-1} \end{bmatrix}, \\
\begin{bmatrix} \mathscr{N}_2^n \\ \mathscr{D}_2^n \end{bmatrix} &= \widetilde{T}_0 \begin{bmatrix} 0 \\ \mathscr{D}_1^{n-1} \end{bmatrix} + T_1 \begin{bmatrix} \mathscr{N}_2^{n-1} \\ \mathscr{D}_2^{n-1} \end{bmatrix} + T_2 \begin{bmatrix} \mathscr{N}_3^{n-1} \\ \mathscr{D}_3^{n-1} \end{bmatrix}, \\
\begin{bmatrix} \mathscr{N}_j^n \\ \mathscr{D}_j^n \end{bmatrix} &= T_0 \begin{bmatrix} \mathscr{N}_{j-1}^{n-1} \\ \mathscr{D}_{j-1}^{n-1} \end{bmatrix} + T_1 \begin{bmatrix} \mathscr{N}_j^{n-1} \\ \mathscr{D}_j^{n-1} \end{bmatrix} + T_2 \begin{bmatrix} \mathscr{N}_{j+1}^{n-1} \\ \mathscr{D}_{j+1}^{n-1} \end{bmatrix}, \text{ for } j = 3,\dots,N-2, \\
\begin{bmatrix} \mathscr{N}_{N-1}^n \\ \mathscr{D}_{N-1}^n \end{bmatrix} &= T_0 \begin{bmatrix} \mathscr{N}_{N-2}^{n-1} \\ \mathscr{D}_{N-2}^{n-1} \end{bmatrix} + T_1 \begin{bmatrix} \mathscr{N}_{N-1}^{n-1} \\ \mathscr{D}_{N-1}^{n-1} \end{bmatrix} + \widetilde{T}_2 \begin{bmatrix} \mathscr{N}_N^{n-1} \\ 0 \end{bmatrix}, \\
\begin{bmatrix} \mathscr{N}_N^n \\ 0 \end{bmatrix} &= \widetilde{T}_1 \begin{bmatrix} \mathscr{N}_N^{n-1} \\ \mathscr{D}_N^{n-1} \end{bmatrix} + \widetilde{T}_2 \begin{bmatrix} \mathscr{N}_{N-1}^{n-1} \\ \mathscr{D}_{N-1}^{n-1} \end{bmatrix},
\end{aligned} \tag{38}$$

where

$$T_0 := \begin{bmatrix} \frac{2}{\gamma_2} & \frac{k\gamma_1}{\gamma_2} \\ 0 & 0 \end{bmatrix},\ T_1 := \begin{bmatrix} 1-\mu & 0 \\ 0 & 1-\theta \end{bmatrix},\ T_2 := \begin{bmatrix} 0 & 0 \\ \frac{-\theta\gamma_1}{k\gamma_2} & \frac{2\theta}{\gamma_2} \end{bmatrix},$$
$$\widetilde{T}_0 := \begin{bmatrix} 0 & \frac{\mu k\gamma_2}{\gamma_1} \\ 0 & 0 \end{bmatrix},\ \widehat{T}_1 := \begin{bmatrix} 0 & 0 \\ 0 & 1-\theta \end{bmatrix},\ \widetilde{T}_1 := \begin{bmatrix} 1-\mu & 0 \\ 0 & 0 \end{bmatrix},\ \widetilde{T}_2 := \begin{bmatrix} 0 & 0 \\ -\frac{\theta\gamma_1}{k\gamma_2} & 0 \end{bmatrix}.$$

Defining $\mathbf{e}^n := \left[0, \mathscr{D}_1^n, \mathscr{N}_2^n, \mathscr{D}_2^n, \dots, \mathscr{N}_j^n, \mathscr{D}_j^n, \dots, \mathscr{N}_{N-1}^n, \mathscr{D}_{N-1}^n, \mathscr{N}_N^n, 0\right]^\top$, the iteration relations (38) may be rewritten as

$$\mathbf{e}^n = T_{2D}^{DN}\mathbf{e}^{n-1},$$

where T_{2D}^{DN} has the same structure as T_{1D}^{DN} given in (37).

Even tough we observe numerically that $\rho(T_{2D}^{DN}) < 1$, one can also verify that in general $\|T_{2D}^{DN}\|_\infty > 1$. Hence, in contrast to the other methods discussed in this paper, the infinity-norm is not suitable to bound the spectral radius and conclude convergence and scalability. Nevertheless in Theorem 5, under certain assumptions and using similarity arguments as in [6], we prove scalability of the PDNM.

Theorem 5 *Denote by $k_{\min}$ the minimum frequency and define $\alpha(x) := 1/\cosh(x)$. If $\theta = \mu$, then*

$$\rho(T_{2D}^{DN}) \le \bar{\rho}(\mu) := \sqrt{1-\mu+\mu^2} + \mu\alpha(k_{\min}L),$$

where $\bar{\rho}(\mu)$ is independent of N. Furthermore, if $\cosh(k_{\min}L) > 2$, then $\bar{\rho}(\mu) < 1$ for any positive μ such that $\mu < \frac{1-2\alpha(k_{\min}L)}{1-\alpha(k_{\min}L)^2}$, which implies that the PDNM is convergent and scalable.

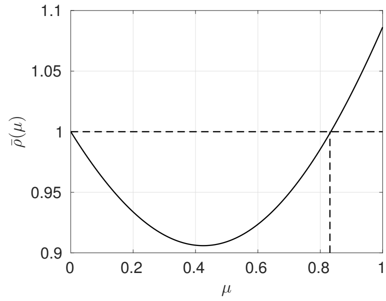

Fig. 10 Function $\mu \mapsto \bar{\rho}(\mu)$ for $L = 1$ and $\widehat{L} = 1$. Notice that for $\mu < 0.831$ (vertical dashed line) it holds that $\bar{\rho}(\mu) < 1$.

We show in Figure 10 the function $\bar{\rho}(\mu)$ for the case $\widehat{L} = 1$, that is $k_{\min} = \pi$. The proof of Theorem 5 relies on the following lemma.

Lemma 3 *Let* $\alpha(x) := 1/\cosh(x)$. *Then for any* $x \in (0, \infty)$ *such that* $\cosh(x) > 2$ *it holds that* $\frac{1-2\alpha(x)}{1-\alpha(x)^2} \in (0,1)$. *Moreover, for any* $x \in (0,\infty)$ *and* $\mu \in (0,1)$ *such that* $\cosh(x) > 2$ *and* $\mu < \frac{1-2\alpha(x)}{1-\alpha(x)^2}$, *it holds that* $\sqrt{1-\mu+\mu^2} + \alpha(x)\mu < 1$.

Proof Let $x \in (0,\infty)$, then $\alpha(x) = 1/\cosh(x) < 1$. Hence we have $0 < 1-\alpha(x)^2 < 1$. Now, take any $x \in (0,\infty)$ such that $\cosh(x) > 2$. First, we have $\frac{1}{2} > \frac{1}{\cosh(x)}$, which implies that $1 - 2\alpha(x) > 0$. Second, we note that $1-2\alpha(x) < 1-\alpha(x) < 1-\alpha(x)^2$. Therefore, we obtain that $\frac{1-2\alpha(x)}{1-\alpha(x)^2} \in (0,1)$. Now take any $\mu \in (0,1)$ such that $\mu < \frac{1-2\alpha(x)}{1-\alpha(x)^2}$. This implies that $1-2\alpha(x) + (\alpha(x)^2-1)\mu > 0$. Multiplying this by μ, with a direct calculation, we get $-\mu+\mu^2 < -2\alpha(x)\mu + \alpha(x)^2\mu^2$. Adding 1 to both sides and taking the square root then leads to the claim.

We are now ready to prove Theorem 5.

Proof If $\mu = \theta$, the matrix T_{2D}^{DN} has the structure

$$
T_{2D}^{DN} := \begin{bmatrix}
0 & & & & & & & & & & \\
& \widetilde{B}_{1,1} & \widetilde{B}_{1,2} & \frac{2\mu}{\gamma_2} & & & & & & & \\
& \widetilde{B}_{2,1} & \widetilde{B}_{2,2} & & & & & & & & \\
& & & \widehat{B}_{1,1} & \widehat{B}_{1,2} & \frac{2\mu}{\gamma_2} & & & & & \\
& & \frac{2\mu}{\gamma_2} & \widehat{B}_{2,1} & \widehat{B}_{2,2} & & & & & & \\
& & & \ddots & \ddots & \ddots & \ddots & & & & \\
& & & & & \widehat{B}_{1,1} & \widehat{B}_{1,2} & \frac{2\mu}{\gamma_2} & & & \\
& & & & \frac{2\mu}{\gamma_2} & \widehat{B}_{2,1} & \widehat{B}_{2,2} & & & & \\
& & & & & & & \overline{B}_{1,1} & \overline{B}_{1,2} & \frac{2\mu}{\gamma_2} & \\
& & & & & & \frac{2\mu}{\gamma_2} & \overline{B}_{2,1} & \overline{B}_{2,2} & & \\
& & & & & & & & & & 0
\end{bmatrix},
$$

where $\widetilde{B}, \widehat{B}, \overline{B} \in \mathbb{R}^{2\times 2}$. We introduce an invertible block diagonal matrix

$$G := \begin{bmatrix} g & 0 & & & & & & \\ 0 & \widetilde{G} & 0 & & & & & \\ & 0 & \widehat{G} & 0 & & & & \\ & & 0 & \widehat{G} & 0 & & & \\ & & & \ddots & \ddots & \ddots & & \\ & & & & 0 & \widehat{G} & 0 \\ & & & & & 0 & g \end{bmatrix}, \text{ with } \widehat{G} := \begin{bmatrix} \widehat{d}_1 & 0 \\ 0 & \widehat{d}_2 \end{bmatrix} \text{ and } \widetilde{G} := \begin{bmatrix} \widetilde{d}_1 & 0 \\ 0 & \widetilde{d}_2 \end{bmatrix},$$

where the elements $g, \widehat{d}_1, \widehat{d}_2, \widetilde{d}_1, \widetilde{d}_2 \in \mathbb{R} \setminus \{0\}$ will be chosen in such a way that the matrix $G^{-1} T_{2D}^{DN} G$ can be bounded in some suitable norm. We have

$$G^{-1} T_{2D}^{DN} G := \begin{bmatrix} 0 & & & & & & & & & \\ & \widetilde{C}_{1,1} & \widetilde{C}_{1,2} & \frac{2\mu}{\gamma_2} & & & & & & \\ & \widetilde{C}_{2,1} & \widetilde{C}_{2,2} & & & & & & & \\ & & & \widehat{C}_{1,1} & \widehat{C}_{1,2} & \frac{2\mu}{\gamma_2} & & & & \\ & & \frac{2\mu}{\gamma_2} & \widehat{C}_{2,1} & \widehat{C}_{2,2} & & & & & \\ & & & \ddots & \ddots & \ddots & \ddots & & & \\ & & & & & \widehat{C}_{1,1} & \widehat{C}_{1,2} & \frac{2\mu}{\gamma_2} & & \\ & & & & \frac{2\mu}{\gamma_2} & \widehat{C}_{2,1} & \widehat{C}_{2,2} & & & \\ & & & & & & & \overline{C}_{1,1} & \overline{C}_{1,2} & \frac{2\mu}{\gamma_2} \\ & & & & & & \frac{2\mu}{\gamma_2} & \overline{C}_{2,1} & \overline{C}_{2,2} & \\ & & & & & & & & & 0 \end{bmatrix},$$

where

$$\widetilde{C} = \widetilde{G}^{-1} \widetilde{B} \widetilde{G}, \quad \widehat{C} = \widehat{G}^{-1} \widehat{B} \widehat{G}, \quad \overline{C} = \widehat{G}^{-1} \overline{B} \widehat{G}.$$

Now, we split $G^{-1} T_{2D}^{DN} G$ into a sum

$$G^{-1} T_{2D}^{DN} G = T_{\text{diag}} + T_{\text{off}},$$

where T_{diag} contains the diagonal blocks, that is

$$T_{\text{diag}} = \begin{bmatrix} 0 & & & & & & \\ & \widetilde{C} & & & & & \\ & & \widehat{C} & & & & \\ & & & \ddots & & & \\ & & & & \widehat{C} & & \\ & & & & & \overline{C} & \\ & & & & & & 0 \end{bmatrix},$$

and $T_{\text{off}} = G^{-1} T_{2D}^{DN} G - T_{\text{diag}}$ contains the remaining off-diagonal elements $\frac{2\mu}{\gamma_2}$. Then we have

$$\begin{aligned} \rho(T_{2D}^{DN}) &= \rho(G^{-1} T_{2D}^{DN} G) \leq \|G^{-1} T_{2D}^{DN} G\|_2 = \|T_{\text{diag}} + T_{\text{off}}\|_2 \\ &\leq \|T_{\text{diag}}\|_2 + \|T_{\text{off}}\|_2 \leq \sqrt{\rho(T_{\text{diag}}^\top T_{\text{diag}})} + \sqrt{\rho(T_{\text{off}}^\top T_{\text{off}})}. \end{aligned} \tag{39}$$

Notice that

$$T_{\text{off}}^\top T_{\text{off}} = \text{diag}\left(0, 0, \frac{4\mu^2}{\gamma_2^2}, \ldots, \frac{4\mu^2}{\gamma_2^2}, 0, 0\right),$$

and hence $\sqrt{\rho(T_{\text{off}}^\top T_{\text{off}})} = \frac{2\mu}{\gamma_2}$. Now, we focus on the term $\rho(T_{\text{diag}}^\top T_{\text{diag}})$. The block diagonal structure of $T_{\text{diag}}^\top T_{\text{diag}}$ allows us to write

$$\rho(T_{\text{diag}}^\top T_{\text{diag}}) = \sqrt{\max\{\rho(\widetilde{C}^\top \widetilde{C}), \rho(\widehat{C}^\top \widehat{C}), \rho(\overline{C}^\top \overline{C})\}}. \tag{40}$$

The evaluation of the spectral radii $\rho(\widetilde{C}^\top \widetilde{C})$, $\rho(\widehat{C}^\top \widehat{C})$, and $\rho(\overline{C}^\top \overline{C})$ leads to the analysis of cumbersome formulas, and we thus bound instead the spectral radii by the corresponding infinity-norms. To do so, setting $\widetilde{d}_1 := \gamma_1$ and $\widetilde{d}_2 := k\gamma_2$, we obtain

$$\rho(\widetilde{C}^\top \widetilde{C}) = \rho(\widetilde{G}\widetilde{B}^\top \widetilde{G}^{-1}\widetilde{G}^{-1}\widetilde{B}\widetilde{G}) \leq \|\widetilde{G}\widetilde{B}^\top \widetilde{G}^{-1}\widetilde{G}^{-1}\widetilde{B}\widetilde{G}\|_\infty = 2\mu^2 - 2\mu + 1.$$

Next, we set $\widehat{d}_1 := \gamma_2$ and $\widehat{d}_2 := k\gamma_1$ and get

$$\begin{aligned}\rho(\widehat{C}^\top \widehat{C}) &= \rho(\widehat{G}\widehat{B}^\top \widehat{G}^{-1}\widehat{G}^{-1}\widehat{B}\widehat{G}) \leq \|\widetilde{G}\widehat{B}^\top \widetilde{G}^{-1}\widetilde{G}^{-1}\widehat{B}\widetilde{G}\|_\infty \\ &= 2\mu^2 - 2\mu + 1 + \frac{4\mu(1-\mu)}{\gamma_2^2} \leq 2\mu^2 - 2\mu + 1 + \frac{4\mu(1-\mu)}{(e^{k_{\min}L} + e^{-k_{\min}L})^2},\end{aligned}$$

where we used that $\gamma_2 = e^{kL} + e^{-kL} \geq e^{k_{\min}L} + e^{-k_{\min}L}$ for any $k \geq k_{\min}$, and

$$\begin{aligned}\rho(\overline{C}^\top \overline{C}) &= \rho(\widehat{G}\overline{B}^\top \widehat{G}^{-1}\widehat{G}^{-1}\overline{B}\widehat{G}) \leq \|\widetilde{G}\overline{B}^\top \widetilde{G}^{-1}\widetilde{G}^{-1}\overline{B}\widetilde{G}\|_\infty \\ &= \max\left\{1-\mu, 1-\mu + \frac{\mu^2(e^{-kL} - e^{kL})^4}{(e^{-kL} + e^{kL})^4}\right\} \leq 1 - \mu + \mu^2,\end{aligned}$$

where the fact that $\frac{(e^{-kL}-e^{kL})^4}{(e^{-kL}+e^{kL})^4} \leq 1$ for any k is used. Now, a direct calculation shows that

$$2\mu^2 - 2\mu + 1 \leq 2\mu^2 - 2\mu + 1 + \frac{4\mu(1-\mu)}{(e^{k_{\min}L} + e^{-k_{\min}L})^2} \leq 1 - \mu + \mu^2,$$

for any $\mu \in (0,1)$. Therefore, we obtain

$$\|T_{\text{diag}}\|_2 = \rho(T_{\text{diag}}^\top T_{\text{diag}}) \leq \sqrt{1 - \mu + \mu^2}.$$

Recalling (39) and (40), we conclude that

$$\begin{aligned}\rho(T_{2D}^{DN}) &\leq \|T_{\text{diag}}\|_2 + \|T_{\text{off}}\|_2 \leq \sqrt{1-\mu+\mu^2} + \frac{2\mu}{\gamma_2} \\ &\leq \sqrt{1-\mu+\mu^2} + \frac{2\mu}{(e^{k_{\min}L} + e^{-k_{\min}L})} =: \bar{\rho}(\mu),\end{aligned}$$

which is first statement of the theorem. The second part follows now from Lemma 3 by observing that if $\bar{\rho}(\mu) < 1$, then $\rho(T_{2D}^{DN}) \leq \bar{\rho}(\mu) < 1$ where $\bar{\rho}(\mu)$ is independent of N.

6 Neumann-Neumann method

In this section, we study the convergence of the Neumann-Neumann method (NNM) as described in [40] for the solution of the two-dimensional problem (4)-(5)[1]. The error equations for NNM are given by the following: first solve

$$\begin{aligned} -\Delta e_j^n &= 0 \text{ in } \Omega_j, \\ e_j^n(\cdot,0) = 0,\ & e_j^n(\cdot,L) = 0, \\ e_j^n(a_{j-1},\cdot) = \mathscr{D}_{j-1}^n,\ & e_j^n(a_j,\cdot) = \mathscr{D}_j^n, \end{aligned}$$

for $j = 2,\dots,N-1$ and

$$\begin{aligned} -\Delta e_1^n &= 0 \text{ in } \Omega_1, & -\Delta e_N^n &= 0 \text{ in } \Omega_N, \\ e_1^n(\cdot,0) = 0,\ & e_1^n(\cdot,L) = 0, & e_N^n(\cdot,0) = 0,\ & e_N^n(\cdot,L) = 0, \\ e_1^n(a_0,\cdot) = 0,\ & e_1^n(a_1,\cdot) = \mathscr{D}_1^n, & e_N^n(a_{N-1},\cdot) = \mathscr{D}_{N-1}^n,\ & e_N^n(a_N,\cdot) = 0, \end{aligned}$$

then solve

$$\begin{aligned} -\Delta \psi_j^n &= 0 \quad \text{in } \Omega_j, \\ \partial_x \psi_j^n(\cdot,0) = 0,\ & \psi_j^n(\cdot,L) = 0, \\ \partial_x \psi_j^n(a_{j-1},\cdot) &= \partial_x e_j^n(a_{j-1},\cdot) - \partial_x e_{j-1}^n(a_{j-1},\cdot), \\ \partial_x \psi_j^n(a_j,\cdot) &= \partial_x e_j^n(a_j,\cdot) - \partial_x e_{j+1}^n(a_j,\cdot), \end{aligned}$$

for $j = 2,\dots,N-1$ and

$$\begin{aligned} -\Delta \psi_1^n &= 0 \quad \text{in } \Omega_1, \\ \psi_1^n(\cdot,0) = 0,\ \psi_1^n(\cdot,L) &= 0,\ \psi_1^n(a_0,\cdot) = 0, \\ \partial_x \psi_1^n(a_1,\cdot) &= \partial_x e_1^n(a_1,\cdot) - \partial_x e_2^n(a_1,\cdot), \end{aligned}$$

and

$$\begin{aligned} -\Delta \psi_N^n &= 0 \quad \text{in } \Omega_N, \\ \psi_N^n(\cdot,0) = 0,\ \psi_N^n(\cdot,L) &= 0,\ \psi_N^n(a_N,\cdot) = 0, \\ \partial_x \psi_N^n(a_{N-1},\cdot) &= \partial_x e_N^n(a_{N-1},\cdot) - \partial_x e_{N-1}^n(a_{N-1},\cdot), \end{aligned}$$

and finally set

$$\mathscr{D}_j^{n+1} := \mathscr{D}_j^n - \vartheta(\psi_{j+1}^n(a_j,\cdot) + \psi_j^n(a_j,\cdot)), \tag{41}$$

for $j = 1,\cdots,N-1$, where $\vartheta > 0$. As in the last sections, we use the Fourier expansion

$$e_j^n(x,y) = \sum_{m=1}^{\infty} v_j^n(x,k)\sin(ky), \quad \psi_j^n(x,y) = \sum_{m=1}^{\infty} w_j^n(x,k)\sin(ky),$$

where $k = \frac{\pi m}{\widehat{L}}$. The Fourier coefficients $v_j^n(x,k)$ and $w_j^n(x,k)$ solve the problems

$$\begin{aligned} k^2 v_j^n - \partial_{xx} v_j^n &= 0 \quad \text{in } (a_{j-1},a_j), & k^2 w_j^n - \partial_{xx} w_j^n &= 0 \quad \text{in } (a_{j-1},a_j), \\ v_j^n(a_{j-1},k) &= \mathscr{D}_{j-1}^n, & \partial_x w_j^n(a_{j-1},k) &= \partial_x v_j^n(a_{j-1},k) - \partial_x v_{j-1}^n(a_{j-1},k), \\ v_j^n(a_j,k) &= \mathscr{D}_j^n, & \partial_x w_j^n(a_j,k) &= \partial_x v_j^n(a_j,k) - \partial_x v_{j+1}^n(a_j,k), \end{aligned}$$

[1] Notice that in 1D the NNM is not well defined because the solution of pure Neumann problems with a non-zero kernel are necessary for the interior subdomains.

for $j=2,\dots,N-1$, and

$$\begin{aligned} k^2 v_1^n - \partial_{xx} v_j^n &= 0 \quad \text{in } (a_0,a_1), & k^2 w_1^n - \partial_{xx} w_1^n &= 0 \quad \text{in } (a_0,a_1),\\ v_1^n(a_0,k) &= 0, & \widetilde{w}_1^n(a_0,k) &= 0,\\ v_1^n(a_1,k) &= \mathscr{D}_1^n, & \partial_x w_1^n(a_1,k) &= \partial_x v_1^n(a_1,k) - \partial_x v_2^n(a_1,k), \end{aligned}$$

and

$$\begin{aligned} k^2 v_N^n - \partial_{xx} v_N^n &= 0 \quad \text{in } (a_{N-1},a_N), & k^2 w_N^n - \partial_{xx} w_N^n &= 0 \quad \text{in } (a_{N-1},a_N),\\ v_N^n(a_{N-1},k) &= \mathscr{D}_{N-1}^n, & \partial_x w_N^n(a_{N-1},k) &= \partial_x v_N^n(a_{N-1},k) - \partial_x v_{N-1}^n(a_{N-1},k),\\ v_N^n(a_N,k) &= 0, & w_N^n(a_N,k) &= 0, \end{aligned}$$

for the first and last subdomains. Setting for simplicity of notation $\mathscr{D}_0^n = \mathscr{D}_N^n = 0$ and defining $\gamma_1 := e^{kL} - e^{-kL}$, the solution v_j^n can be written as

$$v_j^n(x,k) = \frac{1}{\gamma_1}\left[\mathscr{D}_j^n\left(e^{k(x-(j-1)L)} - e^{k((j-1)L-x)}\right) + \mathscr{D}_{j-1}^n\left(e^{k(jL-x)} - e^{k(x-jL)}\right)\right],$$

which is used to solve the problems in w_j^n, and we obtain

$$\begin{aligned} w_j^n(x,k) = &\frac{1}{\gamma_1^2}\left(2\mathscr{D}_{j-1}^n(e^{kL}+e^{-kL}) - 2\mathscr{D}_j^n - 2\mathscr{D}_{j-2}^n\right)\left(e^{k(x-jL)} + e^{k(jL-x)}\right)\\ &+ \frac{1}{\gamma_1^2}\left(2\mathscr{D}_j^n(e^{kL}+e^{-kL}) - 2\mathscr{D}_{j-1}^n - 2\mathscr{D}_{j+1}^n\right)\left(e^{k(x-(j-1)L)} + e^{k((j-1)L-x)}\right), \end{aligned}$$

for $j=2,\dots,N-1$, and

$$\begin{aligned} w_1^n(x,k) &= \frac{1}{\gamma_1\gamma_2}\left(2\mathscr{D}_1^n(e^{kL}+e^{-kL}) - 2\mathscr{D}_2^n\right)\left(e^{kx} - e^{-kx}\right),\\ w_N^n(x,k) &= \frac{1}{\gamma_1\gamma_2}\left(-2\mathscr{D}_{N-1}^n(e^{kL}+e^{-kL}) + 2\mathscr{D}_{N-2}^n\right)\left(e^{k(x-NL)} - e^{k(NL-x)}\right), \end{aligned}$$

362 where $\gamma_2 := e^{kL} + e^{-kL}$. Using equation (41) we get

$$\mathscr{D}_j^{n+1} = \mathscr{D}_j^n - \frac{\vartheta}{\gamma_1^2}\left[4\mathscr{D}_j^n\left(\left(e^{kL}+e^{-kL}\right)^2 - 2\right) - 4\mathscr{D}_{j-2}^n - 4D_{j+2}^n\right], \tag{42}$$

363 for $j=2,\dots,N-2$, and

$$\begin{aligned} \mathscr{D}_1^{n+1} = \mathscr{D}_1^n &- \frac{\vartheta}{\gamma_2}\left(2(e^{kL}+e^{-kL})\mathscr{D}_1^n - 2\mathscr{D}_2^n\right)\\ &- \frac{\vartheta}{\gamma_1^2}\left(2((e^{kL}+e^{-kL})^2-2)\mathscr{D}_1^n + 2(e^{kL}+e^{-kL})\mathscr{D}_2^n - 4\mathscr{D}_3^n\right),\\ \mathscr{D}_{N-1}^{n+1} = \mathscr{D}_{N-1}^n &- \frac{\vartheta}{\gamma_2}\left(2(e^{kL}+e^{-kL})\mathscr{D}_{N-2}^n - 2\mathscr{D}_{N-2}^n\right)\\ &- \frac{\vartheta}{\gamma_1^2}\left(2((e^{kL}+e^{-kL})^2-2)\mathscr{D}_{N-1}^n + 2(e^{kL}+e^{-kL})\mathscr{D}_{N-2}^n - 4\mathscr{D}_{N-3}^n\right). \end{aligned} \tag{43}$$

We define $\mathbf{e}^n = \left[\mathscr{D}_1^n, \mathscr{D}_2^n, \cdots, \mathscr{D}_{N-1}^n\right]^\top$, and write equations (42)-(43) as $\mathbf{e}^{n+1} = T_{2D}^{NN}\mathbf{e}^n$, where the iteration matrix T_{2D}^{NN} is given by

$$T_{2D}^{NN} = \begin{bmatrix} \widetilde{\alpha} & \widetilde{\gamma} & \widetilde{\beta} & & & & & \\ 0 & \alpha & 0 & \beta & & & & \\ \beta & 0 & \alpha & 0 & \beta & & & \\ & \ddots & \ddots & \ddots & \ddots & \ddots & & \\ & & & \ddots & \ddots & \alpha & 0 & \beta \\ & & & & \beta & 0 & \alpha & 0 \\ & & & & & \widetilde{\beta} & \widetilde{\gamma} & \widetilde{\alpha} \end{bmatrix},$$

with $\alpha := 1 - \frac{4\vartheta}{\gamma_1^2}\left(\left(e^{kL}+e^{-kL}\right)^2 - 2\right)$, $\beta := \frac{4\vartheta}{\gamma_1^2}$, $\widetilde{\alpha} := 1 - \frac{2\vartheta}{\gamma_2}(e^{kL}+e^{-kL}) - \frac{2\vartheta}{\gamma_1^2}((e^{kL}+e^{-kL})^2 - 2)$, $\widetilde{\gamma} := \frac{2\vartheta}{\gamma_2} - \frac{2\vartheta}{\gamma_1^2}(e^{kL}+e^{-kL})$, $\widetilde{\beta} := \frac{4\vartheta}{\gamma_1^2}$.

Theorem 6 *If $\frac{L}{\widehat{L}} > \frac{\ln(1+\sqrt{2})}{\pi}$, then the NNM with $\vartheta = \frac{1}{4}$ is scalable, in the sense that $\rho(T_{2D}^{NN}) \leq \|T_{2D}^{NN}\|_\infty = \frac{4}{\gamma_1^2} < 1$.*

Proof The infinity-norm of T_{2D}^{NN} is given by

$$\|T_{2D}^{NN}\|_\infty = \max\left\{|\widetilde{\alpha}| + |\widetilde{\gamma}| + |\widetilde{\beta}|, |\alpha| + 2|\beta|\right\}.$$

Using $\vartheta = \frac{1}{4}$ and exploiting the definition of γ_1, the coefficient α in T_{2D}^{NN} becomes

$$\alpha = 1 - \frac{1}{\gamma_1^2}\left(\left(e^{kL}+e^{-kL}\right)^2 - 2\right) = 1 - \frac{\cosh(kL)^2}{\sinh(kL)^2} + \frac{1}{2}\frac{1}{\sinh(kL)^2} = -\frac{2}{\gamma_1^2}.$$

Similarly, one obtains that $\widetilde{\alpha} = -\frac{1}{\gamma_1^2}$. Moreover, we have $\beta = \widetilde{\beta} = \frac{1}{\gamma_1^2}$. Therefore, we get

$$\|T_{2D}^{NN}\|_\infty = \max\left\{\left(2 + \frac{2}{\gamma_2}\right)\frac{1}{\gamma_1^2}, \frac{4}{\gamma_1^2}\right\} = \frac{4}{\gamma_1^2},$$

since $\gamma_2 > 1$. This shows that $\|T_{2D}^{NN}\|_\infty$ is strictly smaller than one if the condition $\frac{4}{\gamma_1^2} < 1$ holds, meaning that $\gamma_1 > 2$, and since the map $k \mapsto \gamma_1 = 2\sinh(kL)$ is strictly increasing in k, it suffices that $\gamma_1 > 2$ is satisfied for just $k = \frac{\pi}{\widehat{L}}$. Hence the condition becomes $\sinh(kL) > 1$ or equivalently $kL > \operatorname{arcsinh}(1) = \ln(1+\sqrt{2})$, which concludes the proof.

We show in Figure 11 two examples of the spectral radius and the infinity norm of the iteration matrix of NNM for different subdomain heights, which illustrates the strong dependence of NNM on the subdomain height. Note that in Theorem 6 we assumed that $\frac{L}{\widehat{L}} > \frac{\ln(1+\sqrt{2})}{\pi}$. If this condition is not satisfied, numerical experiments show that $\rho(T_{2D}^{NN}) > 1$, and therefore the method is not convergent and can thus not be scalable.

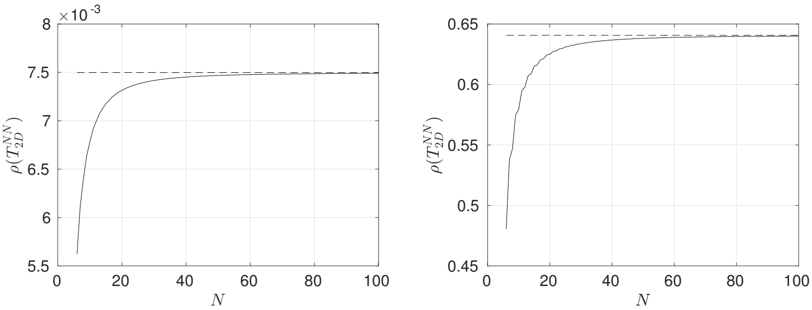

Fig. 11 Spectral radius (solid line) and infinity-norm (dashed line) of T_{2D}^{NN} for $L=1$, $\vartheta=\frac{1}{4}$, and $k=\pi$. Left: $\widehat{L}=1$.*Right* : $\widehat{L}=3$. We see that the subdomain height has a strong influence on the performance.

7 Numerical experiments

We solve numerically problem (4)-(5) with $f_j=0$ and $g_j=0$ by applying the domain-decomposition methods studied in the previous sections. We choose subdomains having height $\widehat{L}=1$ and length $L=1$ (without overlap), that is each subdomain without including the overlap is a unit square. The Laplace operator defined on this square is discretized by the classical 5-point finite-difference stencil defined on a uniform grid with J interior points in both x and y directions, with $J=100$. The mesh size is $h=\frac{1}{J+1}$ and the overlap (for PSM and OSM) is set to $\delta=10h$. The number of (fixed-sized) subdomains is $N=100$. We generate the error sequence $\{e_j^n\}_n$ by applying PSM, OSM, PDNM, and NNM starting with an initial error $e^0(x,y)=\sum_{m=1}^{J}\gamma_m\sin(m\pi y)$, where the coefficients γ_m are randomly chosen in the interval $(-1,1)$ in order to insert error components in all the frequencies. For the OSM the optimized Robin parameter is $p=3.61$, which has been found minimizing the maximum with respect to k of the spectral radii of the matrices T_{2D}^{O}. The relaxation parameters of the PDNM are $\theta=\mu=\frac{1}{2}$, while the relaxation parameter of the NNM is $\theta=\frac{1}{4}$. The iterative procedures are stopped when the error $\|e^n\|_\infty:=\max_j\max_{\Omega_j}|e_j|$ is smaller than the tolerance $\texttt{tol}=10^{-16}$. In Figures 12-13-14-15 (left) we compare the decay of the errors of the 4 methods studied in this paper with the theoretical convergence rate obtained by a numerical estimate of the spectral radii of the transfer matrices T_{2D}, T_{2D}^{O}, T_{2D}^{DN}, and T_{2D}^{NN}.

In particular, the spectral radii are computed using their maximizing frequencies, that is $k=k_{\min}=\pi$ for all the methods. In all cases we observe a very good agreement of the numerical decay (dashed lines) with the theoretical estimate (solid lines). We see also that the NNM requires less iterations (only 7) than all the others to reach the desired tolerance. The OSM requires about 16 iterations to converge, but at each iteration only J subproblems are solved, while the NNM requires the solution of $2J$ subproblems, so their performance is comparable, and in addition, one could use higher order optimized transmission conditions for OSM, see [13], to lower the iteration count further. The PSM and the PDNM converge more slowly, needing about 65 and 110 iterations. Finally, in order to study the scalability of the 4 methods, we repeat the previous experiment with different numbers of fixed-sized subdomains N and different values of tol. The results shown in Figures 12-13-14-15 (right) show that the number of iterations (up to small changes for small values of N) is constant with respect to N. These numerical experiments are in agreement with the theoretical results proved in this paper.

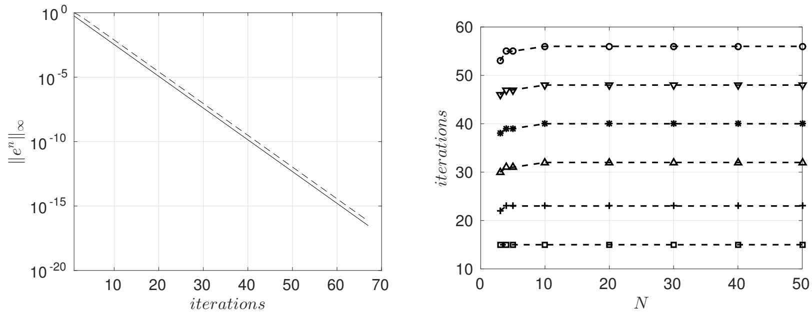

Fig. 12 Left: numerical (dashed line) and theoretical (solid line) decay of the error of the PSM. Right: number of iterations performed as function of the number of subdomains *N*; each curve corresponds to a different fixed tolerance. In particular, from the bottom to the top the curves correspond to tol equal to 10^{-4}, 10^{-6}, 10^{-8}, 10^{-10}, 10^{-12}, 10^{-14}.

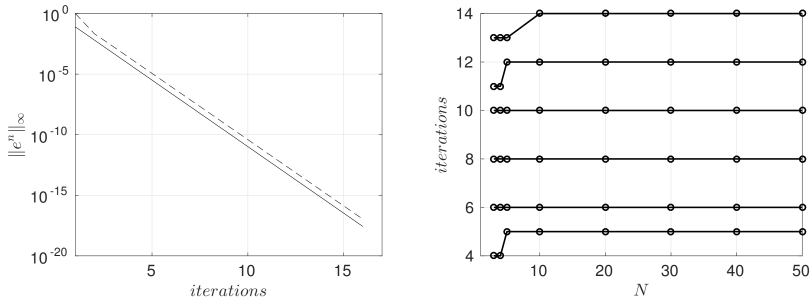

Fig. 13 Left: numerical (dashed line) and theoretical (solid line) decay of the error of the OSM. Right: number of iterations performed as function of the number of subdomains *N*; each curve corresponds to a different fixed tolerance. In particular, from the bottom to the top the curves corresponds to tol equal to 10^{-4}, 10^{-6}, 10^{-8}, 10^{-10}, 10^{-12}, 10^{-14}.

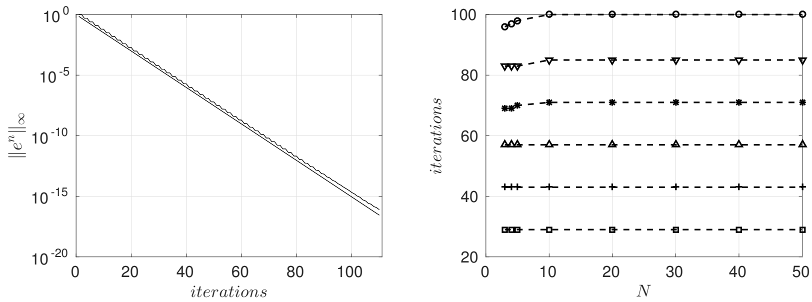

Fig. 14 Left: numerical (dashed line) and theoretical (solid line) decay of the error of the PDNM. Right: number of iterations performed as function of the number of subdomains *N*; each curve corresponds to a different fixed tolerance. In particular, from the bottom to the top the curves corresponds to tol equal to 10^{-4}, 10^{-6}, 10^{-8}, 10^{-10}, 10^{-12}, 10^{-14}.

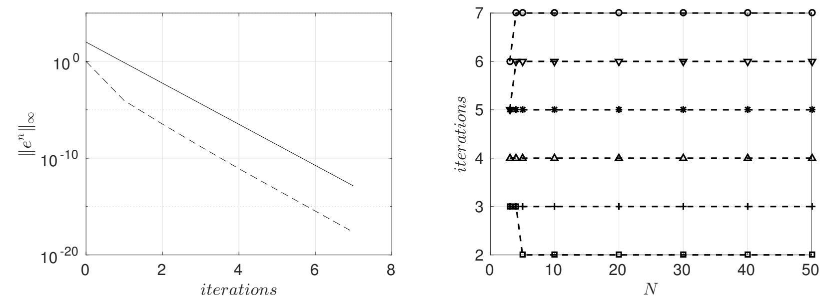

Fig. 15 Left: numerical (dashed line) and theoretical (solid line) decay of the error of the NNM. Right: number of iterations performed as function of the number of subdomains N; each curve corresponds to a different fixed tolerance. In particular, from the bottom to the top the curves corresponds to tol equal to 10^{-4}, 10^{-6}, 10^{-8}, 10^{-10}, 10^{-12}, 10^{-14}.

8 Why the methods scale in 2D but not in 1D

We showed a very different convergence behavior for all one level domain-decomposition methods for the solution of a chain of N fixed-sized subdomains when N increases: the methods for the solution of a one-dimensional chain are not scalable, whereas they are scalable for the solution of a two-dimensional chain. At first glance, the two models seem to be very similar, and we want to give now an intuitive explanation for this different behavior. As we have already discussed in Section 3.1 for the PSM in the one-dimensional case, the propagation of a reduction of the error starts from the first and last subdomains and moves towards the subdomains being in the middle of the chain. Therefore, for some given initial error e^0, one has to wait about $N/2$ iterations before observing a contraction of the error in the middle of the chain. This fact is due to the (only) two homogeneous Dirichlet boundary conditions that are imposed at the extrema $x = a_1$ and $x = b_N$ of the domain Ω, see (6)-(7). Therefore, the "internal subdomains" do not directly benefit from the good effect of these zero Dirichlet conditions. On the other hand, in the two-dimensional case, each subdomain in the chain benefits from the zero Dirichlet conditions imposed at the top and at the bottom of the rectangles Ω_j, see (9)-(10). Therefore, a contraction of the error starts immediately in each subdomain and one has not to wait for the effect coming from the left/right boundaries of Ω to propagate into the entire chain to reach a given tolerance. Hence, the "distributed" homogeneous Dirichlet boundary condition in the two-dimensional case is the reason for the scalability of the PSM, and this argument is also valid for the other domain decomposition methods we discussed.

Remark 1 If we have Neumann boundary conditions on the top and bottom boundaries of the two dimensional problem, then PSM, OSM and PDNM do not scale, as one can see by slightly adapting our analysis: the Neumman boundary condition implies the use of a cosine Fourier series, instead of the sine Fourier series. The zero frequency is now included in the expansion, i.e. $e_j^n(x,y) = \sum_{m=0}^{\infty} v_j^n(x,k_m)\cos(k_m y)$. For $m = 0$, the Fourier coefficient v_0^n satisfies the same equation as in the one dimensional case, and thus the scalability property of the two dimensional case is lost due to the presence of this frequency, since the spectral radius of the corresponding matrix deteriorates as the number of subdomains grows. For the one level NNM the situation is even worse: NNM is not well posed then, since the second step of the iteration would require the solution of pure Neumann problems for interior subdomains, as in 1D.

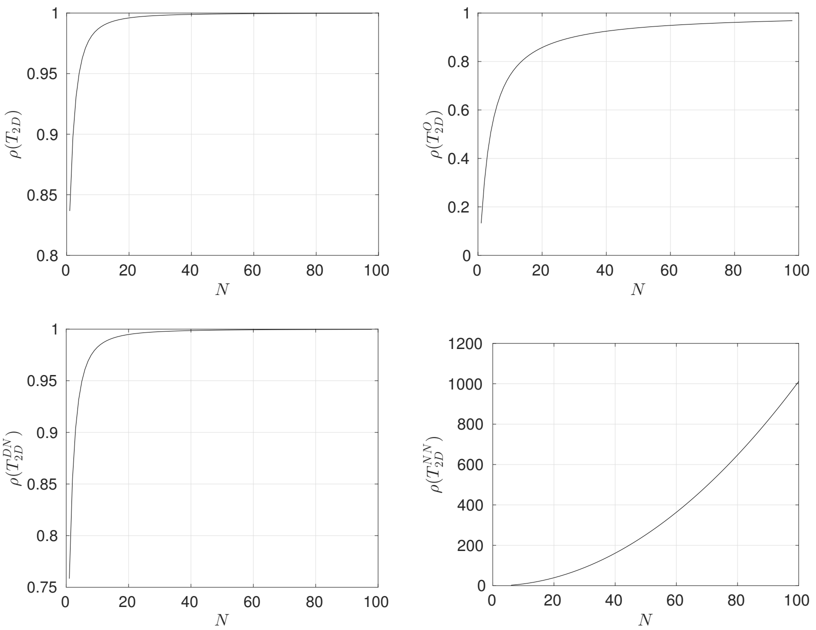

Fig. 16 Spectral radii of the iteration matrices for the different methods corresponding to $L = 1/N$, $\widehat{L} = 1$, and $k = \pi$. For PSM and OSM the overlap is rescaled as $\delta = L/10$.

Remark 2 Our analysis can also be used to recover by a numerical evaluation of the convergence factors the well-known results concerning the non scalability of one level domain decomposition methods for fixed-size problems, where the subdomains become smaller and smaller as their number grows, see for instance [40]: by setting $L = 1/N$ and increasing the number of subdomains, we see that the convergence factors of the classical and optimized Schwarz methods and the Dirichlet-Neumann methods tend to 1 when the subdomain number increases, as shown in Figure 16. So these methods can not be weakly scalable in this setting, in contrast to the case where the subdomain size remains fixed, as in the earlier sections. For the Neumann-Neumann method, the situation is even worse, since the assumption of Theorem 6 is not satisfied anymore, and the method fails to converge when the number of subdomains grows in this case.

Remark 3 As an anonymous referee suggested, it is interesting to also consider the case of a fixed number of multiple vertical layers of chains. In this case, the methods would still be scalable when adding more and more subdomains in the horizontal direction, provided the subdomain size remains fixed. This can be seen as follows: for a single layer of N subdomains, we have seen that the contraction reaches the middle subdomain after $\frac{N}{2}$ iterations. To use this argument in the vertical direction, suppose for example that we have 5 vertical layers: if we then consider 3 iterations, then the contraction given by the Dirichlet boundary condition on the top and bottom reaches the middle layer, and thus all layers start contracting. So looking in packets of 3 iterations, the errors will contract independently of how many subdomains are added in the horizontal direction in each layer, due to our results for a single layer.

References

1. V. Barone and M. Cossi. Quantum calculation of molecular energies and energy gradients in solution by a conductor solvent model. *The Journal of Physical Chemistry A*, 102(11):1995–2001, 1998.
2. P. E Bjørstad and O. B. Widlund. Iterative methods for the solution of elliptic problems on regions partitioned into substructures. *SIAM Journal on Numerical Analysis*, 23(6):1097–1120, 1986.
3. E. Cancès, Y. Maday, and B. Stamm. Domain decomposition for implicit solvation models. *The Journal of Chemical Physics*, 139:054111, 2013.
4. F. Chaouqui and M. J. Gander. Optimal coarse spaces for FETI and their approximation. *accepted in ENUMATH 2017 Proceedings*, 2018.
5. F. Chaouqui, M. J. Gander, and K. Santugini-Repiquet. On nilpotent subdomain iterations. In *Domain Decomposition Methods in Science and Engineering XXIII*, pages 125–133. Springer, Cham, 2017.
6. G. Ciaramella and M. J. Gander. Analysis of the parallel Schwarz method for growing chains of fixed-sized subdomains: Part I. *SIAM J. Num. Anal.*, 55(3):1330–1356, 2017.
7. G. Ciaramella and M. J. Gander. Analysis of the parallel Schwarz method for growing chains of fixed-sized subdomains: Part II. *SIAM J. Num. Anal.*, 56(3):1498–1524, 2018.
8. G. Ciaramella and M. J. Gander. Analysis of the parallel Schwarz method for growing chains of fixed-sized subdomains: Part III. *to appear in ETNA*, 2018.
9. V. Dolean, M. J. Gander, and L. Gerardo-Giorda. Optimized Schwarz methods for Maxwell's equations. *SIAM Journal on Scientific Computing*, 31(3):2193–2213, 2009.
10. Maksymilian Dryja and Olof B. Widlund. *Multilevel additive methods for elliptic finite element problems*. New York University, Department of Computer Science, Courant Institute of Mathematical Sciences, 1990.
11. O. Dubois, M. J. Gander, S. Loisel, A. St-Cyr, and D. B. Szyld. The optimized Schwarz method with a coarse grid correction. *SIAM Journal on Scientific Computing*, 34(1):A421–A458, 2012.
12. C. Farhat, M. Lesoinne, and K. Pierson. A scalable dual-primal domain decomposition method. *Numerical Linear Algebra with Applications*, 7(7-8):687–714, 2000.
13. M. J. Gander. Optimized Schwarz methods. *SIAM Journal on Numerical Analysis*, 44(2):699–731, 2006.
14. M. J. Gander. Schwarz methods over the course of time. *ETNA. Electronic Transactions on Numerical Analysis*, 31:228–255, 2008.
15. M. J. Gander and O. Dubois. Optimized Schwarz methods for a diffusion problem with discontinuous coefficient. *Numerical Algorithms*, 69(1):109–144, 2015.
16. M. J. Gander and L. Halpern. Méthodes de décomposition de domaine. *Encyclopédie électronique pour les ingénieurs*, 2012.
17. M. J. Gander, L. Halpern, and K. Santugini. Discontinuous coarse spaces for DD-methods with discontinuous iterates. In *Domain Decomposition Methods in Science and Engineering XXI*, pages 607–615. Springer, 2014.
18. M. J. Gander, L. Halpern, and K. Santugini. A new coarse grid correction for RAS/AS. In *Domain Decomposition Methods in Science and Engineering XXI*, pages 275–283. Springer, 2014.
19. M. J. Gander, L. Halpern, and K. Santugini. On optimal coarse spaces for domain decomposition and their approximation. In *Domain Decomposition Methods in Science and Engineering XXVI*. Springer, 2018.
20. M. J. Gander and A. Loneland. *SHEM: An optimal coarse space for RAS and its multiscale approximation*, pages 313–321. Springer International Publishing, Cham, 2017.
21. M J Gander, A. Loneland, and T. Rahman. Analysis of a new harmonically enriched multiscale coarse space for domain decomposition methods. *arXiv preprint arXiv:1512.05285*, 2015.
22. M. J. Gander, F. Magoules, and F. Nataf. Optimized Schwarz methods without overlap for the Helmholtz equation. *SIAM Journal on Scientific Computing*, 24(1):38–60, 2002.
23. M. J. Gander and M. Neumüller. Analysis of a new space-time parallel multigrid algorithm for parabolic problems. *SIAM Journal on Scientific Computing*, 38(4):A2173–A2208, 2016.
24. M. J. Gander and B. Song. Complete, optimal and optimized coarse spaces for Additive Schwarz. In *Domain Decomposition Methods in Science and Engineering XXVI*. Springer, 2017.
25. M. J. Gander and T. Vanzan. Heterogeneous optimized Schwarz methods for coupling Helmholtz and Laplace equations. *accepted in Domain Decomposition Methods in Science and Engineering XXIV*, 2018.
26. M. J. Gander and T. Vanzan. Optimized Schwarz methods for advection diffusion equations in bounded domains. *accepted in ENUMATH 2017 Proceedings*, 2018.
27. Walter Gander, Martin J. Gander, and Felix Kwok. *Scientific computing-An introduction using Maple and MATLAB*, volume 11. Springer Science & Business, 2014.
28. C. Japhet, F. Nataf, and F. Rogier. The optimized order 2 method: application to convection–diffusion problems. *Future generation computer systems*, 18(1):17–30, 2001.

29. A. Klamt and G. Schuurmann. COSMO: a new approach to dielectric screening in solvents with explicit expressions for the screening energy and its gradient. *J. Chem. Soc., Perkin Trans. 2*, pages 799–805, 1993.
30. Axel Klawonn and Oliver Rheinbach. Highly scalable parallel domain decomposition methods with an application to biomechanics. *ZAMM-Journal of Applied Mathematics and Mechanics/Zeitschrift für Angewandte Mathematik und Mechanik*, 90(1):5–32, 2010.
31. P.-L. Lions. On the Schwarz alternating method. I. *First international symposium on domain decomposition methods for partial differential equations*, pages 1–42, 1988.
32. P.-L. Lions. On the Schwarz alternating method. II. *Domain Decomposition Methods*, pages 47–70, 1989.
33. P.-L. Lions. On the Schwarz alternating method. III: a variant for nonoverlapping subdomains. In *Third international symposium on domain decomposition methods for partial differential equations*, volume 6, pages 202–223. SIAM Philadelphia, PA, 1990.
34. F. Lipparini, G. Scalmani, L. Lagardère, B. Stamm, E. Cancès, Y. Maday, J.-P. Piquemal, M. J Frisch, and B. Mennucci. Quantum, classical, and hybrid QM/MM calculations in solution: General implementation of the ddCOSMO linear scaling strategy. *The Journal of chemical physics*, 141(18):184108, 2014.
35. F. Lipparini, B. Stamm, E. Cances, Y. Maday, and B. Mennucci. Fast domain decomposition algorithm for continuum solvation models: Energy and first derivatives. *Journal of Chemical Theory and Computation*, 9(8):3637–3648, 2013.
36. F. Nataf, F. Rogier, and E. de Sturler. *Optimal interface conditions for domain decomposition methods*. École polytechnique, 1994.
37. Roy A Nicolaides. Deflation of conjugate gradients with applications to boundary value problems. *SIAM Journal on Numerical Analysis*, 24(2):355–365, 1987.
38. A. Quarteroni and A. Valli. *Domain Decomposition Methods for Partial Differential Equations*. Numerical Mathematics and Scientific Computation. Clarendon Press, 1999.
39. Barry Smith, Petter Bjorstad, and William Gropp. *Domain decomposition: parallel multilevel methods for elliptic partial differential equations*. Cambridge university press, 2004.
40. A. Toselli and O. Widlund. *Domain Decomposition Methods: Algorithms and Theory*, volume 34. Springer, 2005.
41. T. N. Truong and E. V. Stefanovich. A new method for incorporating solvent effect into the classical, ab initio molecular orbital and density functional theory frameworks for arbitrary shape cavity. *Chemical Physics Letters*, 240(4):253–260, 1995.